

Redshift-distance Survey of Early-type Galaxies: the ENEARc Cluster Sample ¹

M. Bernardi², M. V. Alonso³, L. N. da Costa^{4,5}, C. N. A. Willmer^{5,6}

G. Wegner⁷, P. S. Pellegrini⁵, C. Rit e⁵, M. A. G. Maia⁵

ABSTRACT

This paper presents data on the ENEARc subsample of the larger ENEAR survey of the nearby early-type galaxies. The ENEARc galaxies belong to clusters and were specifically chosen to be used for the construction of a $D_n - \sigma$ template. The ENEARc sample includes new measurements of spectroscopic and photometric parameters (redshift, velocity dispersion, line index Mg_2 , and the angular diameter d_n) as well as data from the literature. New spectroscopic data are given for 229 cluster early-type galaxies and new photometry is presented for 348 objects. Repeat and overlap observations with external data sets are used to construct a final merged catalog consisting of 640 early-type galaxies in 28 clusters. Objective criteria, based on catalogs of groups of galaxies derived from complete redshift surveys of the nearby universe, are used to assign galaxies to clusters. In a companion paper these data are used to construct the template $D_n - \sigma$ distance relation for early-type galaxies which has been used to estimate galaxy distances and derive peculiar velocities for the ENEAR all-sky sample.

Subject headings: cosmology: observations – galaxies: large-scale structure – galaxies: clustering

²The University of Chicago, 5640 South Ellis Avenue, Chicago, IL 60637, USA

³Observatorio Astronómico de Córdoba, Laprida 854, Córdoba, 5000, Argentina

⁴European Southern Observatory, Karl-Schwarzschild Strasse 2, D-85748 Garching, Germany

⁵Departamento de Astronomia, Observatório Nacional, Rua General José Cristino 77, Rio de Janeiro, R. J., 20921, Brazil

⁶UCO/Lick Observatory, University of California, 1156 High Street, Santa Cruz, CA 95064, USA

⁷Department of Physics & Astronomy, Dartmouth College, Hanover, NH 03755-3528, USA

¹Based on observations at Complejo Astronómico El Leoncito (CASLEO), operated under agreement between the Consejo Nacional de Investigaciones Científicas de la República Argentina and the National Universities of La Plata, Córdoba and San Juan; Cerro Tololo Interamerican Observatory (CTIO), operated by the National Optical Astronomical Observatories, under AURA; European Southern Observatory (ESO), partially under the ESO-ON agreement; Fred Lawrence Whipple Observatory (FLWO); Observatório do Pico dos Dias, operated by the Laboratório Nacional de Astrofísica (LNA); and the MDM Observatory on Kitt Peak.

1. Introduction

For many years cosmic flows have been a promising way to probe mass density fluctuations on intermediate scales ($\lesssim 100h^{-1}$ Mpc) and to obtain dynamical measures of the cosmological parameters. Unfortunately, compiling peculiar velocity data with the desired sky coverage and full sampling is time-consuming, so most previous cosmic flow studies have been based on sparse or non-uniform catalogs, leading to conflicting interpretations. Recently, new large redshift-distance surveys of spiral (SFI; da Costa et al. 1996, Haynes et al. 1999a, 1999b) and early-type galaxies (ENEAR; da Costa et al. 2000a, hereafter Paper I; Wegner et al. 2002; Alonso et al. 2002) have been completed and some of the unresolved issues are being re-addressed with these significantly larger and more uniform samples.

The ENEAR catalog of peculiar velocities described in Paper I is an all-sky catalog which includes a magnitude-limited sample of early-type galaxies (ENEARm) extracted from completed magnitude-limited redshift surveys, as well as a subsample of cluster galaxies which are fainter than the magnitude limit of the parent redshift surveys. The ENEAR catalog is a compilation of observational parameters for ~ 2000 early-type galaxies. It includes new photometric and spectroscopic data for ~ 1500 early-type galaxies in clusters and in the field as well as data from previous work. Our new photometric and spectroscopic measurements are presented in Alonso et al. (2002) and Wegner et al. (2002), respectively. Data from this catalog have already been used in some previous analyses presented in other papers of this series (Bernardi et al. 1998; Borgani et al. 2000; da Costa et al. 2000b; Nusser et al. 2001; Zaroubi et al. 2001).

In conducting these analyses we have found it necessary operationally to split the ENEAR catalog into two samples, ENEARm and ENEARc (see Paper I). The ENEARc is composed of galaxies from ENEARm that are in clusters, but with the addition of galaxies fainter than the original ENEARm magnitude limit using new observations and data in the literature.

The purpose of the present paper is to focus on the ENEARc cluster subsample; here we describe the assignment of galaxies to clusters, the homogenization of our new data with those of previous work, and report the final combined photometric and spectroscopic parameters of the cluster galaxies. The construction of the ENEARc catalog is needed in order to obtain an accurate template scaling relation (the $D_n - \sigma$ relation) which can be used to measure distances and peculiar velocities for all the early-type galaxies in the ENEAR catalog. The $D_n - \sigma$ scaling relation, originally introduced by Dressler et al. (1987), is essentially equivalent to the more general Fundamental Plane (FP, Djorgovski & Davis 1987) defined by early-type galaxies.

The underlying assumption in estimating distances is that these scaling relations are the same for field and cluster galaxies. For galaxies which are at approximately the same redshift, so effects of evolution can be neglected, the dependence of these scaling relations on cluster properties has been investigated by several authors (e.g., Jørgensen, Franx, & Kjørgaard 1996; D’Onofrio et al. 1997; Pahre, Djorgovski, & de Carvalho 1998; Scodreggio et al. 1998; Gibbons, Fruchter, & Bothun 2001; Colless et al. 2001). (For how the FP depends on cluster redshift see e.g., Jørgensen et al. 1999; Treu et al. 1999, 2001; van Dokkum et al. 2001.) Other issues that bear on the results are the assignment of galaxies to clusters, the small number of observed galaxies per cluster, which requires the use of all available cluster data for the definition of a template distance relation, and the possible biases of the parameters resulting from selection effects and measurement errors.

The data presented in this paper are used in Bernardi et al. (2002) to derive the template-distance relation from which the galaxy distances and the peculiar velocity field of the ENEAR sample were derived.

The outline of this paper is as follows: In Section 2 we describe the selection of clusters and the criteria

used for membership assignment. In Section 3 we present the new spectroscopic and photometric data and discuss the corrections applied to our measurements and to those of other authors which bring the available data into a common system. Section 4, contains the final merged and standardized ENEARc catalog of early-type cluster galaxies used to construct the distance relation and peculiar velocity analyses. A brief summary is given in Section 5.

2. Cluster Sample

2.1. Selection

A key requirement for constructing any distance relation based on cluster/group galaxies is to have a well defined procedure for identifying bound systems and assigning galaxies to them. With currently available optical, all-sky redshift surveys (e.g., Huchra et al. 1983, CfA1; Falco et al. 1999, CfA2; da Costa et al. 1988, SSRS; da Costa et al. 1998, SSRS2; Santiago et al. 1995, ORS) a significant improvement can be made on earlier work which justifies reexamining galaxy assignments to clusters.

In this paper we have adopted the following procedure: Clusters within $\sim 10000 \text{ kms}^{-1}$ were selected from group catalogs derived by applying the objective group-finding algorithm of Huchra & Geller (1982) to all complete, magnitude-limited redshift surveys currently available. For most of the sky (~ 6.5 steradians) rich groups ($\gtrsim 15$ members) were drawn from the CfA1 (Geller & Huchra 1983) and SSRS (Maia, da Costa & Latham 1989) catalogs. At low galactic latitudes the catalogs were complemented by groups identified in the Optical Redshift Survey (Santiago et al. 1995). Over the fraction of the sky surveyed by the CfA2 and SSRS2 (~ 4.2 steradians, including more than a third of both galactic caps), we used groups identified by Ramella, Pisani, & Geller (1997) in the CfA2 and Ramella et al. (2002) in the SSRS2, instead of those identified in earlier shallower surveys. This selection is not uniform over the sky because of the different magnitude-limits and density contrast thresholds that had to be adopted in the group identification. An attempt to minimize this effect and include possible fainter members is discussed in Section 2.3.

The final catalog contains 32 rich (> 15 members), 318 medium-size (5-15 members) and 628 small (< 5 members) systems making a total of 978 groups. For each group the combined catalog provides: the number of members; center coordinates, heliocentric radial velocity, velocity dispersion, and the physical size expressed by the pair radius R_p (Ramella, Geller, & Huchra 1989) which is used below to establish cluster membership. The physical parameters of the groups are computed considering all morphological types. Groups with at least 15 members were cross-identified with the Abell and the ACO cluster catalogs (Abell 1958; Abell, Corwin & Olowin 1989). All but three, consisting predominantly of spirals were known clusters. Because of the limiting magnitudes of the parent redshift surveys some faint early-type galaxies, known to be in clusters, are missed by this procedure. Fainter early-types with data in the literature were added to our compilation (See Section 2.3).

To this list we added five additional well-studied clusters: A539, AS639, and A3381 (Jørgensen, Franx, & Kjærgaard 1995a, 1995b) and 7S21 and A347 (Smith et al. 1997). These clusters were excluded from our original list because they are either located at low galactic latitudes, outside the regions probed by the redshift surveys, or because the member galaxies are fainter than the limiting magnitude of these redshift surveys. A special procedure was also adopted to handle the Centaurus cluster, which has two distinct components (Lucey & Carter 1988) but is identified as a single large system in the group catalog. In this case, we assigned memberships based on the observed redshift distribution along the line-of-sight. The resulting list of members for each system agrees well with Lucey & Carter (1988). The physical characteristics of these

two groups, hereafter Cen30 and Cen45, were computed after splitting the systems (see Section 2.2).

From the cluster/group sample above we selected 58 groups containing a minimum of five early-type galaxies and at least 15 members of any morphological type, to provide a reliable cluster velocity dispersion estimate. Figure 1 shows the projected distribution in galactic coordinates of all the 58 selected clusters, including the 28 clusters considered in the present paper. The apparent deficiency of clusters at low galactic latitudes may not be real. However the apparent underdensity of galaxies shown on the left side of the plot at higher galactic latitudes can also be seen in Figure 14 of Paper I, which shows this for the ENEAR and SFI galaxies. We ultimately focused on creating a large database of measurements in common with other authors, and to enlarge the sample of available galaxies in the 28 previously studied clusters.

It is useful to refer to Figure 4 of Paper I, which compares the distribution of clusters on the sky with that of the underlying galaxies. Four clusters lie inside the Perseus-Pisces (PP) region ($0^h < \alpha < 4^h$ and $+20^\circ < \delta < +45^\circ$; Smith et al. 1997). The two dominant concentrations of galaxies, the Great Attractor (GA) and Perseus-Pisces superclusters, are indicated in that figure. Paper I also shows that in our sample, the GA and PP superclusters produce a prominent peak at $\sim 5000 \text{ kms}^{-1}$ in the redshift distribution of the clusters, indicating that our clusters probe the most prominent structures in the nearby universe.

2.2. Properties of the Cluster Sample

The main physical characteristics of the 28 selected clusters are given in Table 1: the cluster name in column (1); columns (2) and (3) give the right ascension and declination, as determined from the group finding algorithm or taken from the references listed in column 9; column (4) is the heliocentric radial velocity; column (5) the cluster velocity dispersion; column (6) the value of the radius R_p , whenever available (see Section 2.3); column (7) the number of early-type galaxies with distances in this paper; column (8) indicates clusters using only measurements obtained by other authors; and column (9) references previous studies of these clusters. Note that the cluster global parameters such as redshift, velocity dispersion, and size were taken from the merged group catalog described earlier. Comparing these redshifts with those obtained using only the cluster early-types, we find insignificant differences, the mean offset being $\sim 20 \text{ kms}^{-1}$ and the scatter $\sim 110 \text{ kms}^{-1}$. The cluster velocity dispersions listed in the table also agree well, with a mean difference of $\sim 40 \text{ kms}^{-1}$ and a scatter of $\sim 130 \text{ kms}^{-1}$. In the latter case, we find that for rich clusters, the values listed in the table are smaller with an offset of $\lesssim 200 \text{ kms}^{-1}$.

Poor sampling of the cluster region affects both the estimated cluster velocity dispersion and the characteristic size scale R_p . In some cases the coordinates of the groups/clusters had to be revised because closer inspection showed that the group catalog was unable to separate neighboring clusters (e.g., A2199/97, Cen30/45) or because groups based on shallow surveys do not faithfully represent the center of the cluster after fainter members have been included (e.g., Klemola 44). Groups found at the edge of a redshift survey tend to have their global parameters affected; in particular the size, as originally listed in the group catalog, can differ. For example, the group radius of Pavo II depends on the density threshold. This may also explain structure found in Doradus. These problems should be kept in mind when investigating correlations that depend on the global cluster parameters such as size and velocity dispersion.

2.3. Membership Assignment

As mentioned in Section 2.1, the group catalogs were derived from redshift surveys with differing limiting magnitudes and selection criteria. To make the distribution of our clusters/groups more uniform across the sky we added other systems in regions of the sky not covered by the redshift surveys. Also, we have increased the number of cluster/group members by including early-type galaxies observed by other authors, below the magnitude limit of the redshift surveys. We have also checked other authors’ membership assignments. A galaxy was assigned to a cluster if it satisfied two conditions. The first condition is $d \leq 1.5R_p$, where d is the distance relative to the group center, determined from the group finding algorithm, and R_p is the group pair radius (both are in h^{-1} Mpc, where $h = H_0/100 \text{ kms}^{-1} \text{ Mpc}^{-1}$). We fixed R_p to $1 h^{-1}$ Mpc for Cen45, not identified by the finding algorithm, for Pavo II at the edge of the redshift survey, and for the five clusters added from the literature.

The second condition is $|cz - cz_{cl}| \leq 1.5\sigma_{cl}$ where cz is the radial velocity of the galaxy, cz_{cl} and σ_{cl} are the systemic velocity and velocity dispersion of the group, respectively. This second requirement does not precisely represent the region within the caustic which marks the boundary of a cluster in redshift space (e.g., Kaiser 1987; Regős & Geller 1989), but the small number of galaxies per cluster and the caustic’s dependence on Ω makes a more precise determination untenable.

To better approximate the real assignment of galaxies to the cluster we also define a class of “peripheral” objects, the criteria depending on the richness of the cluster. For the richest clusters (e.g., Virgo and Coma), “peripheral” galaxies are those which satisfy one of two conditions: $d \leq R_p$ and $1.5\sigma_{cl} \leq |cz - cz_{cl}| \leq 3\sigma_{cl}$, or $1.5R_p \leq d \leq 3R_p$ and $|cz - cz_{cl}| \leq \sigma_{cl}$, while for clusters with fewer members the second condition becomes $1.5R_p \leq d \leq 2R_p$. These conditions are intended to represent the region in redshift-space occupied by cluster members. Applying these criteria, increases the sample of the early-type galaxies by about 20%. When two clusters are close to each other as in the cases of A2199/97 and Cen30/45 ambiguous cases remain. The impact of these objects on the distance relation is discussed in more detail in Bernardi et al. (2002).

Figure 2 shows examples of the resulting projected distribution of objects in and around two of the clusters (similar plots for the other clusters are available; interested readers should contact the first author of this paper directly). The dashed circle corresponds to the angular size of $1.5R_p$ at the cluster redshift. Some systems are well sampled by the available redshift surveys (e.g., Coma, A1367, Virgo, Fornax, Eridanus, Doradus), while at low galactic latitude clusters/groups are only covered by the shallow ORS. The density of galaxies abruptly changes south of -40° , the southern limit of the SSRS2. From these projected distributions, we also found that some group centers, in the group catalogs, are not good estimates. This is the case, e.g., for Pisces, HMS0122+3305, A2199, and the nearby groups such as Eridanus and Doradus, but correcting the central positions leaves the galaxy assignments unaltered. We also find that Klemola 44 may be a superposition of two systems.

Overall $\lesssim 90\%$ of the early-type galaxies assigned to these groups have distances. There are 733 early-type galaxies assigned to the 28 selected clusters/groups (hereafter the ENEARc catalog), of which 640 galaxies have velocity dispersions and d_n measurements, where d_n is the apparent diameter at a given isophotal level, as required to build the $D_n - \sigma$ relation. Of these, 495 satisfy the most stringent membership criteria, whereas 145 are “peripheral” cluster objects. According to our adopted criteria, 15 galaxies assigned to the selected cluster sample by previous authors are non-members.

These non-member galaxies are listed in Table 2, where: column (1) is the name of the galaxy; columns (2) and (3) are the equatorial coordinates; column (4) is the heliocentric redshift; column (5) is the total

magnitude m_B ; column (6) is the name of the cluster to which the galaxy is assigned; column (7) is the pair radius R_p of the cluster; column (8) is the cluster velocity dispersion; column (9) is the projected distance of the galaxy from the cluster center, computed using the angular separation and the cluster redshift; column (10) is the difference between the galaxy and cluster redshifts; and column (11) references previous work. The information on the individual galaxies and groups comes from the literature and the original group catalogs, respectively. Note that Willmer et al. (1991) had already pointed out that [WFC91] 056 and ESO 384G037 are interlopers in AS753, while Jørgensen (1997) noted that D75 and [WFC91] 039 were not members of A194 and AS753, respectively. The galaxies in Table 2 are, therefore, excluded from the ENEARc sample.

Figure 3 summarizes the measured parameters for early-type cluster galaxies. This figure shows the distribution of: redshift (panel a); σ (panel b); Mg_2 index (panel c); and the photometric parameter d_n (panel d). The data include both our measurements and those of other authors calibrated onto a common system as described in the next section.

3. Homogenization of the Measurements

In addition to our all-sky ENEAR redshift-distance survey, over the years we have gathered a large number of spectroscopic and photometric observations of early-type galaxies in clusters with the following three goals in mind: 1) increase the number of galaxies in clusters to improve the statistical accuracy of distance relations; 2) measure many galaxies observed by other authors, in order to scale the available data into a common system and estimate our external errors; 3) obtain repeat observations to estimate our internal errors on a run-by-run basis. Repeat measurements also provide a way to eliminate disparate measurements and improve the statistical error per galaxy. Since a non-negligible number of galaxies, mostly in clusters, had modern high-quality measurements available in the literature, we concentrated our efforts in clusters already studied by other authors.

In the following sections we describe the procedures adopted for homogenizing and combining the spectroscopic and photometric parameters which come from various sources.

3.1. Spectroscopic Data

Details of the observations, data reductions, parameter and error estimates obtained by the ENEAR team are presented in Wegner et al. (2002). The velocity dispersion was measured in the interval 4770 – 5770 Å. Therefore, our estimates do not include the effects of the NaD line which, because of interstellar absorption, could affect the velocity dispersion measurement (e.g., Dressler 1984). It is known that for any given S/N and instrumental resolution, there is a lower limit on the velocity dispersion measurable without introducing significant bias (e.g., Bender 1990). The instrumental resolution of the setups used by the ENEAR team range from 70 kms^{-1} to 100 kms^{-1} . We tested the reliability of the low velocity dispersion measurements by using: a) internal repeated observations, and b) simulations of synthetic noisy “galaxy” spectra (Wegner et al. 2002). The scatter (15 %) given by internal comparisons at low velocity dispersions ($< 70 \text{ kms}^{-1}$) is comparable with the errors (10 %-15 %) associated with those measurements. Simulated “galaxy” spectra, obtained by broadening the spectrum of a template star by Gaussians of different velocity dispersion and by adding different noise, show that for spectra with $S/N > 20$ per pixel the velocity dispersion can be measured reliably down to a value of ~ 65 % of the instrumental resolution. These results show that our random errors are reliable and that our velocity dispersion measurements are not biased—even for values

which are smaller than the instrumental resolution. However, the above tests do not take into account about possible systematic effects due to e.g., template and galaxy mismatches or continuum subtraction problems.

In this section we describe the homogenization procedure for the ENEARc data which include our new measurements as well as data from the literature. The first step in homogenizing the velocity dispersions and line indices is to define a “fiducial” system to which all other measurements can be compared and converted. To achieve this we first brought our measurements onto the same internal system. The ENEAR observations were chosen as this standard system because they are a large (~ 2000) homogeneous set of measurements, which was designed to extensively overlap with other samples and our own individual observing runs. The ENEAR observations were brought into a consistent system as described by Wegner et al. (2002). Briefly, the following procedure was used: we determined a mean offset, Δ , between each galaxy in a given run and all the other runs. We then averaged over all galaxies in a run, weighting by the number of available pairs which yields Δ for that run. We then subtracted Δ from data in each run and repeat the process until no run has an offset above a predefined tolerance. We found no evidence for a more complicated correction for the data. The internal comparisons of the final redshift, velocity dispersion, and the Mg_2 index were found to be in good agreement, showing no systematic trends, and only small zero-point offsets.

The mean redshift offset is $\lesssim 25 \text{ kms}^{-1}$ with a scatter of $\lesssim 40 \text{ kms}^{-1}$; in the case of the velocity dispersion, $\Delta \log \sigma$ is always less than 0.025 and has a scatter of $\lesssim 0.060$ dex. The mean $\Delta \log \sigma$ offset is 0.012 ± 0.008 dex. Finally, the line index Mg_2 has a mean zero-point offset of $\lesssim 0.015 \pm 0.006$ dex with a scatter of ~ 0.020 dex. The velocity dispersions and the values of the Mg_2 index were aperture-corrected to $2r_{norm} = 1.19h^{-1} \text{ kpc}$ (Wegner et al. 2002).

The second step, after calibrating our measurements to a consistent system, was to convert published data to our reference system. An aperture correction consistent with our raw data was made before calibrating them to our “fiducial” system by a zero-point shift, using a procedure similar to the one above. Zero-point corrections were only applied for those data sets for which the offset was larger than its error. Table 3 summarizes the results of this comparison of our data with those of other authors: in column (1) the source of published data; in column (2) the number of velocity dispersion measurements involved in the comparison; in column (3) the offset applied to each set of velocity dispersion measurements; in column (4) the rms value of the differences in the comparison; columns (5)-(7) show the same for the Mg_2 line index. All differences are computed as “our-minus-literature”. The comparisons listed in the table include only cluster galaxies except for the 7S sample; for that sample we also compared the measurements of field galaxies. This was done to increase the accuracy of the comparison.

In total we have 248 measurements of the velocity dispersion and 156 of the Mg_2 index in common with the literature. The external comparisons reported in the table show that the external offsets are, in general, comparable to the mean offset found from our internal comparisons. The measurements obtained by other authors were converted to our “fiducial” system by adding the offsets listed in Table 3. In order to evaluate the final merged and standardized catalog of early-type galaxies a comparison has been made between different (calibrated) measurements of the same galaxy. The results are shown in Figure 4 for those datasets for which direct comparisons are available. The data sets of Lucey et al. (1997) and Smith et al. (1997) have very few galaxies in common with our sample. Therefore, for these two data sets we had to rely on an indirect calibration. This was carried out by using the overlap between the data of these two papers with those of the literature converted directly into our system. Figure 5 shows the result of this indirect calibration.

Figure 6 shows a histogram of the difference between our redshifts and the literature. The mean and

rms scatter of the distribution are $1 \pm 8 \text{ kms}^{-1}$ and 69 kms^{-1} , respectively. Since the typical error in the radial velocity is of the order of $\sim 50 \text{ kms}^{-1}$ we conclude that no correction is required for the redshift measurements.

The spectroscopic data in the ENEARc catalog are summarized in Table 4 which gives: in column (1) the source of measurements; in column (2) the number of new measurements obtained by our team; in column (3) the number of galaxies for which spectroscopic parameters were measured; in column (4) the number of galaxies for which there is only one source; in columns (5)–(7) the same information for the Mg_2 line index. In estimating the contribution of each author we tried to consider only independent measurements, although this is not always possible because some authors combined their new data with previous work. The number of measurements in the table reported for the authors refers only to galaxies in the ENEAR database (see Paper I).

Table 4 shows that we obtained 338 measurements of the velocity dispersion for 229 galaxies and similar numbers for the Mg_2 index; about one-third of our observations have repeats. Using these data, we obtained new distances and Mg_2 indices for ~ 90 galaxies, thereby enlarging the sample of early-type galaxies that can be used in the construction of the $D_n - \sigma$ relation. About 55% of the cluster sample still relies on single velocity dispersion measurements but most of these are now based on high-quality modern observations.

3.2. Photometric Data

Details of the photometric observations are given in Alonso et al. (2002). The same homogenization procedure described above was adopted for the photometric parameter d_n . Following the 7S, d_n is the angular diameter of a circular aperture within which the average integrated surface brightness of a galaxy is equal to a specified value. In our case the angular diameter d_n is measured at the R -band isophotal level of $\mu_R = 19.25 \text{ mag arcsec}^{-1}$. This value roughly corresponds to the value adopted by the 7S in the B -band, assuming a mean color of $(B - R) = 1.5 \text{ mag}$. The light profiles were corrected for the effects of seeing (e.g., Saglia et al. 1997), flux calibrated and corrected for Galactic extinction (Burstein & Heiles 1984). Alonso et al. 2002 show that, for the galaxies in our sample, the Burstein & Heiles extinction corrections agree well with the values derived using the extinction maps of Schlegel, Finkbeiner & Davis (1998). The K-correction and cosmological surface brightness dimming correction were also applied.

As in the case of the spectroscopic parameters, a homogeneous dataset is required. This is particularly important for combining photometric parameters since these come from a variety of sources, many using different filters. To calibrate the photometric parameter d_n to the “fiducial” system, we first checked the internal consistency of our data by comparing the surface brightness profiles of galaxies for which we have more than one observation. For these objects, the dispersion among different measurements was found to be small ($\sim 0.05 \text{ mag/arcsec}^2$ over an interval of typically 3 magnitudes), showing that our reduction and calibration procedures lead to uniform results (see Figure 3.6, 3.7, and 3.8 in Bernardi 1999). We also compared our measures of the surface brightness profiles with those in previous works. This was done to estimate if differences in the zero-point of the photometric calibration, or variations in the filters/colors used by different sources could contribute to the differences observed in the d_n parameter. We found that the comparisons of our surface brightness profiles with those of other sources do not show any systematic gradient or statistically significant offset (see Figure 3.4 in Bernardi 1999). These results justify our choice of applying simple offsets in homogenizing the d_n parameter. As before, our observations were used to define the reference system; we brought the measurements to a common system by minimizing the mean

differences in the d_n derived from galaxies observed in more than one run. The required corrections to bring the measurements into a common system were relatively small: $\Delta \log d_n \lesssim 0.010 \pm 0.004$ dex with a rms scatter of $\lesssim 0.022$ dex (Alonso et al. 2002).

The measurements available in the literature were calibrated to our internal reference system by applying the offsets listed in Table 5, if the offset is larger than its error. This table summarizes the results of the comparison between our data and those of other authors listing: in column (1) the source of published data; in column (2) the number of measurements involved in the comparison; in column (3) the difference between our measurements and those in the literature; and in column (4) the rms value of these differences. There are 379 d_n measurements in common with the literature. The required corrections are small and the scatter compares with that obtained from our internal comparisons, suggesting that one can safely combine the measurements from different data sets. These comparisons are shown in Figure 7 after each individual data set was calibrated to the fiducial system. The agreement is good, with the dispersion being generally smaller than 0.02 dex. Furthermore, there is no evidence of systematic trends, justifying our use of single offsets to bring all of the published data into a common system. As for the spectroscopic parameters, the comparison with the 7S sample also includes field galaxies.

The photometric data assembled for the ENEARc sample are summarized in Table 6 where we list: in column (1) the source of measurements; in column (2) the passband in which the data were measured; in column (3) the number of new measurements including repeat observations; in column (4) the number of galaxies with measured photometric parameters; and in column (5) the number of galaxies for which there is only one source. We have measured 508 d_n for a total of 348 ENEARc galaxies, of which 117 had no previous measurements. About 48% of the cluster sample still relies on single measurements, making the cross-comparison between different sources extremely important.

4. The ENEARc Catalog

As a final result, we have assembled a sample of 640 early-type galaxies in 28 clusters with redshift, velocity dispersion, d_n measurements and, whenever possible, the Mg_2 line index using the membership criteria described above. Of these galaxies, 495 are considered cluster members and 145 “peripheral” objects. All 640 objects were individually inspected and 188 galaxies were removed due to peculiarities and/or problems on their images and/or their spectra (e.g., residual contamination from nearby galaxies or stars; presence of spiral arms or bar; dust lane; high D/B ; emission lines; low S/N) that could affect the measurement of their photometric and spectroscopic parameters.

Table 7 tabulates the main measured parameters for the 452 galaxies suitable for constructing the $D_n - \sigma$ relation and Table 8 contains the 188 cluster galaxies eliminated from further consideration, respectively. For each cluster these tables give: in column (1) the name of the galaxy; in columns (2) and (3) the 1950.0 equatorial coordinates; in column (4) the morphological T type following Lauberts & Valentijn (1989); in column (5) the total B -band magnitude m_B taken from the literature; in column (6) the number of redshift and velocity dispersion measurements obtained from our new data; in column (7) the number of redshift and velocity dispersion measurements available in the literature; in columns (8) and (9) the heliocentric redshift and its error; in columns (10) and (11) the logarithm of the velocity dispersion measurement and its error; in columns (12) and (13) the number of Mg_2 line index measurements available from our new data and from the literature; and in columns (14) and (15) the value and error of the Mg_2 line index. Similarly, columns (16)-(19) give the same information for the photometric parameter $\log d_n$ (d_n in 0.1 arcmin). In addition,

Table 8 gives (column 20) a reference to the Notes to the table indicate the reason(s) for removing the galaxy from the ENEARc sample. The parameters listed in these tables are combined values obtained from the error-weighted mean of the individual measurements using a 3σ -clipping.

5. Summary

In this paper we present spectroscopic (redshift, velocity dispersion, and Mg_2 index) and photometric (d_n) data for 640 galaxies in 28 clusters comprising our ENEARc catalog. The assignment of galaxies to groups and clusters was based on a compilation of objectively identified groups derived from complete redshift surveys of the nearby universe. Roughly 2% of the galaxies were previously assigned to clusters erroneously. The data presented here are a combination of 338 new spectroscopic measurements of 229 galaxies, and 508 new R -band images of 348 galaxies, in addition to those taken from the literature. The large number of galaxies in common with other authors, permits all data to be calibrated into one reference system. Bernardi et al. (2002) use 452 galaxies of ENEARc to determine the $D_n - \sigma$ relation used for ENEAR.

In a forthcoming paper we intend to also measure the FP parameters for the ENEARc galaxies in order to build a template relation for nearby clusters which will serve as a reference for similar studies at high redshift. It is important to point out that the present sample can be significantly expanded by using currently available wide-field imagers and multi-object spectrographs such as 6dF (<http://www.aao.gov.au/ukst/6df.html>) and it may be well worth the effort.

The authors would like to thank the referee for all the helpful comments and all of those who have contributed directly or indirectly to this long-term project. Our special thanks to Otávio Chaves for his many contributions over the years. We would also like to thank D. Burstein, M. Davis, A. Milone, M. Ramella, R. Saglia, and B. Santiago for useful discussions and input. MB thanks the Sternwarte München, the Technische Universität München, ESO Studentship program, and MPA Garching for their financial support during different phases of this research. MVA thanks CNPq for different fellowships at the beginning of the project and the CfA and ESO’s visitor programs for support of visits. MVA is partially supported by CONICET and SecyT. LNdc would like to extend his special thanks to David W. Latham who played a pivotal role at the early stages of this project. GW is grateful to the Alexander von Humboldt-Stiftung for making possible a year’s stay at the Ruhr-Universität in Bochum, and to ESO for support for visits to Garching. Financial support for this work has been given through FAPERJ (CNAW, MAGM, PSSP), CNPq grants 201036/90.8, 301364/86-9 (CNAW), 301366/86-1 (MAGM); NSF AST 9529098 and 0071198 (CNAW); ESO Visitor grant (CNAW). PSP and MAGM thank CLAF for financial support and CNPq fellowships. Most of the observations carried out at ESO’s 1.52m telescope at La Silla were conducted under the auspices of the bi-lateral time-sharing agreement between ESO and MCT/Observatório Nacional. We are grateful to the anonymous referee whose detailed comments greatly improved this paper.

REFERENCES

- Abell, 1958 ApJS, 3, 211
- Abell, G. O., Corwin, H. G., Jr. & Olowin, R. P. 1989, ApJS, 70, 1
- Alonso, M. V., Bernardi, M., Wegner, G. et al. 2002, in preparation
- Bender, R. 1990, A&A, 229, 441
- Bernardi, M., Renzini, A., da Costa, L. N., Wegner, G., Alonso, M. V., Pellegrini, P. S., Rit e, C. & Willmer, C. N. A. 1998, ApJL, 508, 143
- Bernardi, M. 1999, PhD Thesis, Ludwig-Maximilian Universit at, M nchen
- Bernardi, M., Alonso, M. V., da Costa, L. N., et al. 2002, AJ, in press
- Borgani, S., Bernardi, M., da Costa, L. N., Wegner, G., Alonso, M. V., Willmer, C. N. A., Pellegrini, P. S., & Maia, M. A. G. 2000, ApJL, 537, 1
- Burstein, D. & Heiles, C. 1984, ApJS, 54, 33
- Colless, M., Saglia, R. P., Burstein, D., Davies, R. L., McMahan, R. K., & Wegner, G. 2001, MNRAS, 321, 277
- da Costa, L.N., Pellegrini, P.S., Sargent, W.L.W, Tonry, J., Davis, M., Meiksin, A., Latham, D.W., Menzies, J.W., & Coulson, I. A., 1988, ApJ, 327, 544
- da Costa, L. N., Freudling, W., Wegner, G., Giovanelli, R., Haynes, M.P. & Salzer, J. J. 1996, ApJL, 468, 5
- da Costa, L., Willmer, C. N. A., Pellegrini, P. S. et al., 1998, AJ, 116, 1 (Paper I)
- da Costa, L. N., Bernardi, M., Alonso, M. V., Wegner, G., Willmer, C. N. A., Pellegrini, P. S., Rit e, C., & Maia, M. A. G. 2000a, AJ, 120, 95
- da Costa, L. N., Bernardi, M., Alonso, M. V., Wegner, G., Willmer, C. N. A., Pellegrini, P. S., Maia, M. A. G., & Zaroubi, S. 2000b, ApJL, 537, 81
- Djorgovski, S. & Davis, M. 1987, Ap. J., 313, 59
- D’Onofrio, M., Capaccioli, M., Zaggia, S. R. & Caon, N. 1997, MNRAS, 289, 847
- Dressler, A. 1984, ApJ, 286, 97
- Dressler, A. 1987, ApJ, 317, 1
- Dressler, A., Lynden-Bell, D., Burstein, D., Davies, R. L., Faber, S. M., Terlevich, R. J. & Wegner, G. 1987, ApJ, 313, 42
- Dressler, A., Faber, S. M. & Burstein, D. 1991, ApJ, 368, 54
- Faber, S. M., Wegner, G., Burstein, D., Davies, R. L., Dressler, A., Lynden-Bell, D., & Terlevich, R. J. 1989, ApJS, 69, 763
- Falco, E. E., Kurtz, M. J., Geller, M. J., Huchra, J. P., Peters, J., Berlind, P., Mink, D. J., Tokarz, S. P. & Elwell, B., 1999, PASP, 111, 438

- Geller, M. J. & Huchra, J. P. 1983, *ApJS*, 52, 61
- Gibbons, R. A., Fruchter, A. S. & Bothun, G. D. 2001, *AJ*, 121, 649
- Haynes, M. P., Giovanelli, R., Salzer, J. J., Wegner, G., Freudling, W., da Costa, L. N., Herter, T. & Vogt, N. P. 1999a, *AJ*, 117, 1668
- Haynes, M. P., Giovanelli, R., Chamaraux, P., da Costa, L. N., Freudling, W., Salzer, J. J. & Wegner, G. 1999b, *AJ*, 117, 2039
- Huchra, J., Davis, M., Latham, D. & Tonry, J., 1983, *ApJS*, 52, 89
- Huchra, J. P. & Geller, M. J. 1982, *ApJ* 257, 423
- Jørgensen, I., Franx, M. & Kjaergaard, P. 1995a, *MNRAS*, 273, 1097
- Jørgensen, I., Franx, M. & Kjaergaard, P. 1995b, *MNRAS*, 276, 1341
- Jørgensen, I., Franx, M., & Kjaergaard, P. 1996, *MNRAS*, 280, 167
- Jørgensen, I. 1997, *MNRAS*, 288, 161
- Jørgensen, I., Franx, M., Hjorth, J., & van Dokkum, P. G. 1999, *MNRAS*, 308, 833
- Kaiser, N. 1987, *MNRAS*, 227, 1
- Lauberts, A. & Valentijn, E. A. 1989, in *The Surface Photometry Catalogue of the ESO-Uppsala Galaxies* (Garching: ESO)
- Lucey, J. R. & Carter, D. 1988, *MNRAS* 235, 1177
- Lucey, J. R., Guzmán, R., Steel, J. & Carter, D. 1997, *MNRAS*, 287, 899
- Maia, M. A. G., da Costa, L. N. & Latham, D. W. 1989, *ApJS*, 69, 809
- Nusser, A., da Costa, L. N., Branchini, E., Bernardi, M., Alonso, M. V., Wegner, G., Willmer, C. N. A., & Pellegrini, P. S. 2001, *MNRAS* 320, 21
- Pahre, M.A., Djorgovski, S.G., & de Carvalho, R.R. 1998, *AJ*, 116, 1606
- Ramella, M., Geller, M. J., & Huchra, J. P. 1989, *ApJ*, 344, 57
- Ramella, M., Pisani, A., & Geller, M. J. 1997, *AJ*, 113, 483
- Ramella, M., et al., 2002, in preparation
- Regös, E., & Geller, M.J. 1989, *AJ*, 98, 755
- Saglia, R. P., Bertschinger, E., Baggley, G., Burstein, D., Colles, M., Davies, R. L., McMahan, Jr., R. K. & Wegner, G. 1997, *ApJS* 109, 79
- Santiago, B. X., Strauss, M. A., Lahav, O., Davis, M., Dressler, A., & Huchra, J. P. 1995, *ApJ*, 446, 457
- Schlegel, D. J., Finkbeiner, D. P., & Davis, M. 1998, *ApJ*, 500, 525
- Scodreggio, M., Gavazzi, G., Belsole, E., Pierini, D., & Boselli, A. 1998, *MNRAS*, 301, 1001

- Smith, R. J., Lucey, J. R., Hudson, M. J. & Steel, J. 1997, MNRAS, 291, 461
- Treu, T., Stiavelli, M., Casertano, S., Møller, P., & Bertin, G. 1999, MNRAS, 308, 1037
- Treu, T., Stiavelli, M., Bertin, G., Casertano, S., & Møller, P. 2001, MNRAS, 326, 237
- van Dokkum, P. G., Franx, M., Kelson, D. D., & Illingworth, G. D. 2001, ApJL, 553, 39
- Wegner, G., Colless, M., Saglia, R. P., McMahan, R. K., Davies, R. L., Burstein, D., & Bagglely, G. 1999, MNRAS, 305, 259
- Wegner, G., Willmer, C. N. A., Bernardi, M. et al., 2002, in preparation
- Willmer, C. N., Focardi, P., da Costa, L. N., & Pellegrini, P. S. 1989, AJ, 98, 1531
- Willmer, C. N., Focardi, P., Chan, R., Pellegrini, P. S. & da Costa, L. A. 1991, AJ 101, 57
- Zaroubi, S., Bernardi, M., da Costa, L. N., Hoffman, Y., Alonso, M. V., Wegner, G., Willmer, C. N. A., & Pellegrini, P. S. 2001, MNRAS, 326, 375

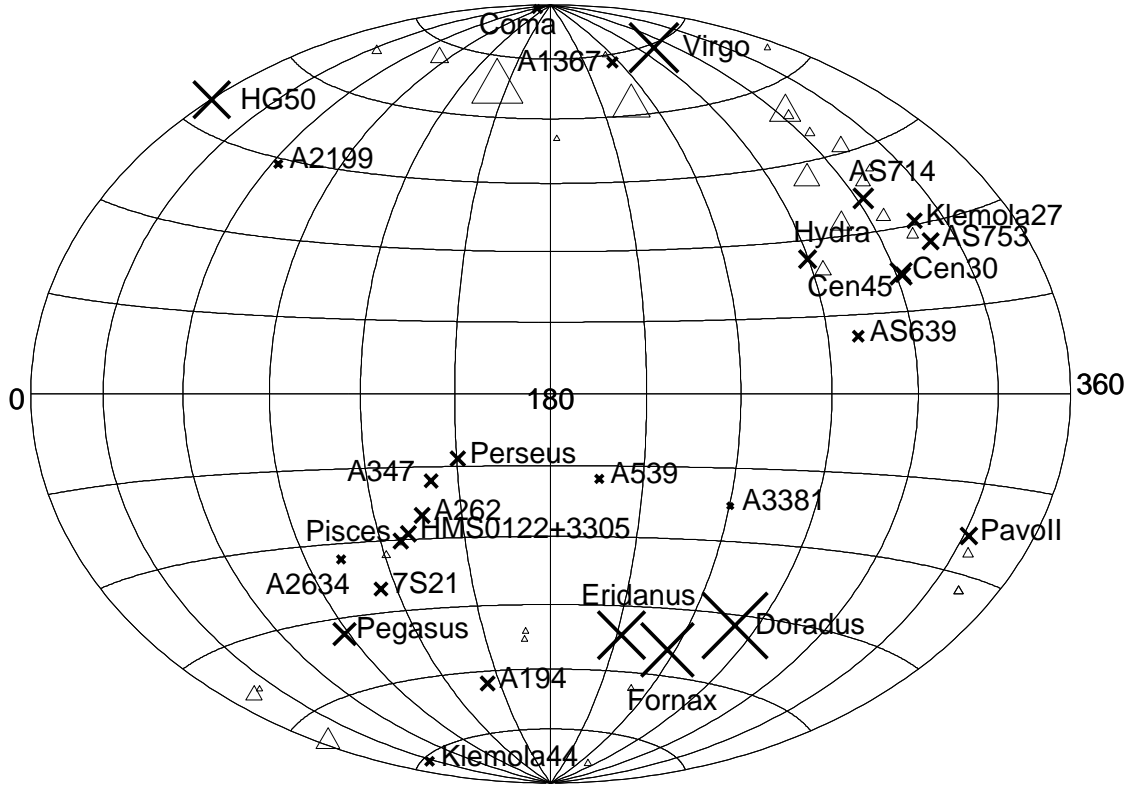


Fig. 1.— The spatial distribution in galactic coordinates of all the 58 cluster/groups with characteristics suitable for the determination of the distance relation (see text). The 28 clusters used in the present paper are shown as crosses. The size of the symbols is inversely proportional to the cluster redshift.

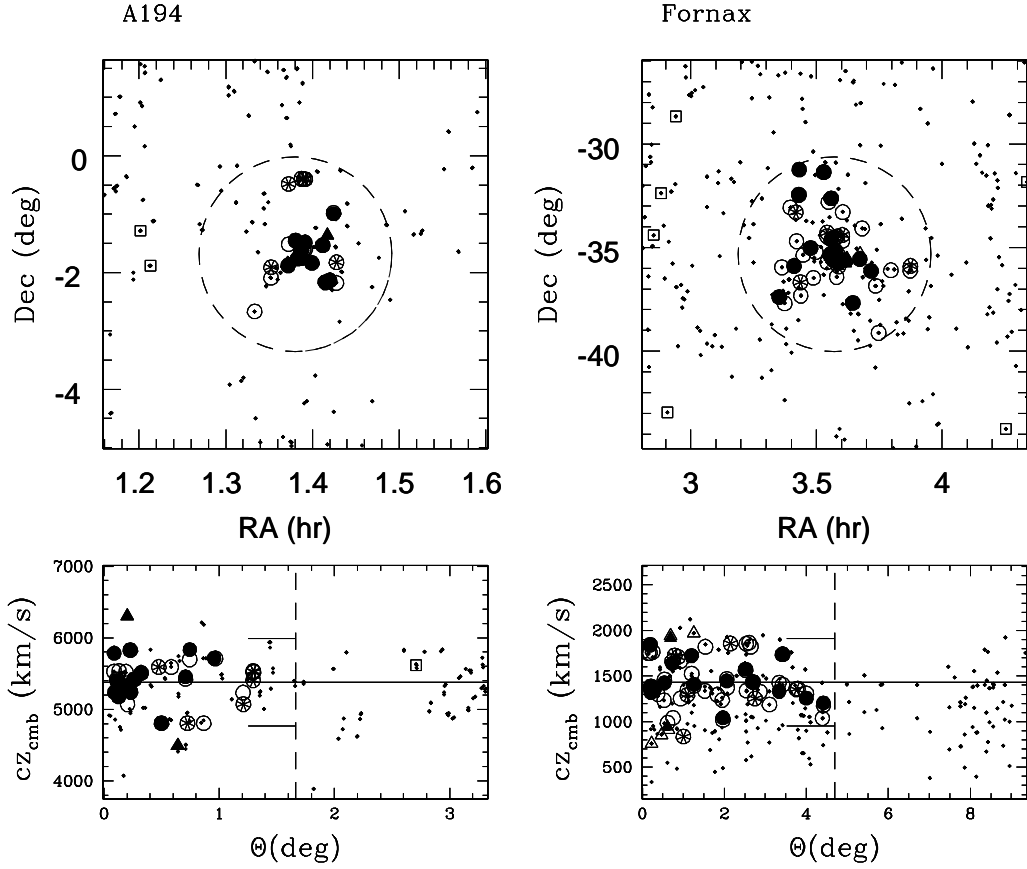


Fig. 2.— Examples of the distribution of galaxies, in the equatorial coordinate system (upper panel), and the radial velocity versus angular distance from the cluster center (lower panel) for two clusters. Shown are: late-type field galaxies taken from the available redshift surveys (small dots) and early-type field galaxies in the ENEAR catalog (open squares); cluster early-type galaxies with (filled and skeletal circles) or without measured distances (open circles). The skeletal symbol represents “discarded” galaxies (see the text and Table 2 for details); and “peripheral” galaxies with (filled triangles) or without measured distances (open triangles).

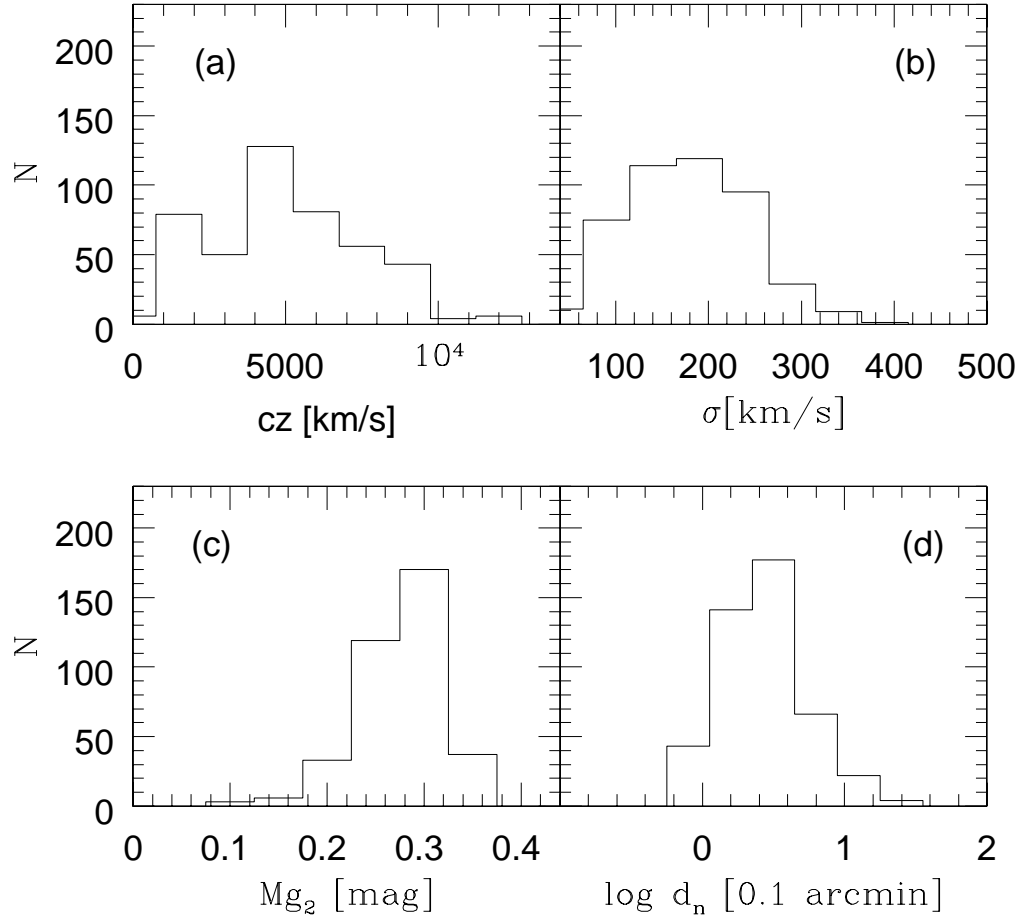


Fig. 3.— The distribution of spectroscopic and photometric parameters for the ENEARc galaxies: upper panels (a) redshift and (b) velocity dispersion; lower panels (c) Mg_2 line index and (d) the photometric parameter $\log d_n$.

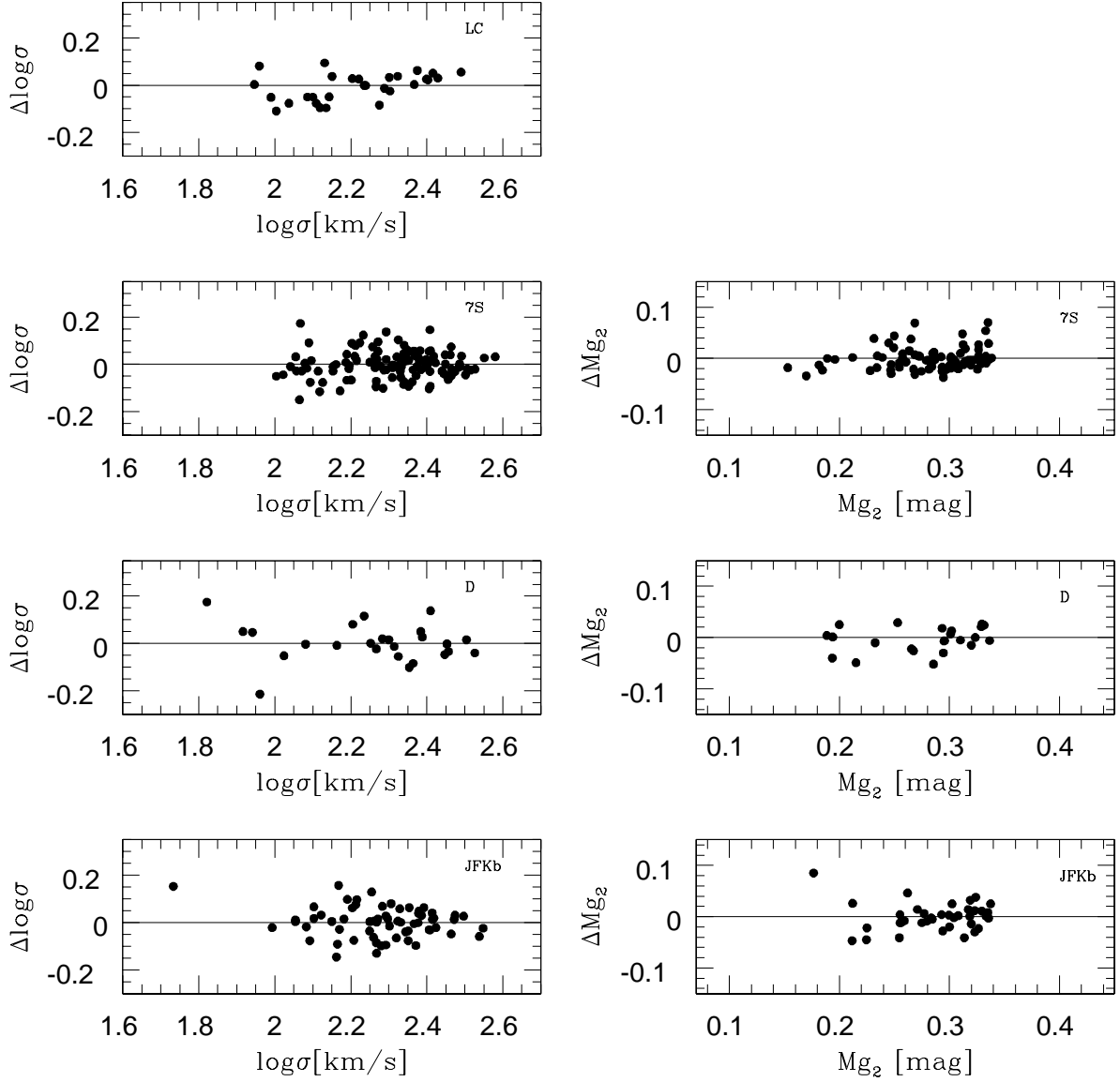


Fig. 4.— Comparison of our measurements with those of other authors. Different panels show the comparison for each individual source: Lucey & Carter (1988) (LC); Faber et al. (1989) (7S); Dressler (1987) and Dressler, Faber, & Burstein (1991) (D); and Jørgensen et al. (1995b) (JFKb).

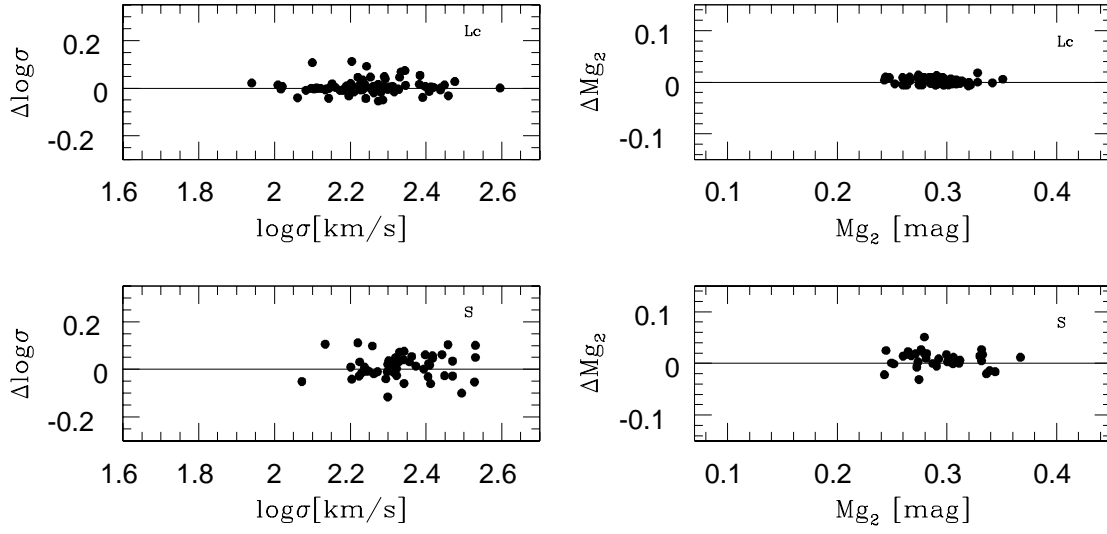


Fig. 5.— Comparison between measurements from different authors for which no direct calibration was possible (Lucey et al. 1997 (Lc) and Smith et al. 1997 (S)) after bringing all measurements into a common system.

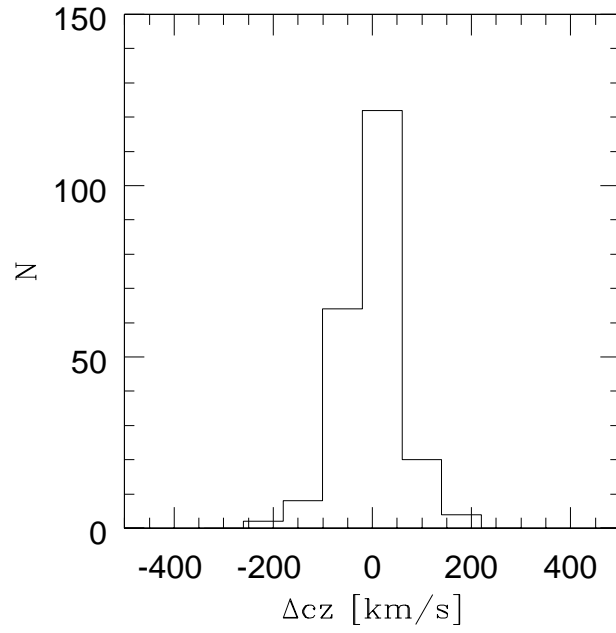


Fig. 6.— The distribution of the redshift difference between our measurements and those from the literature.

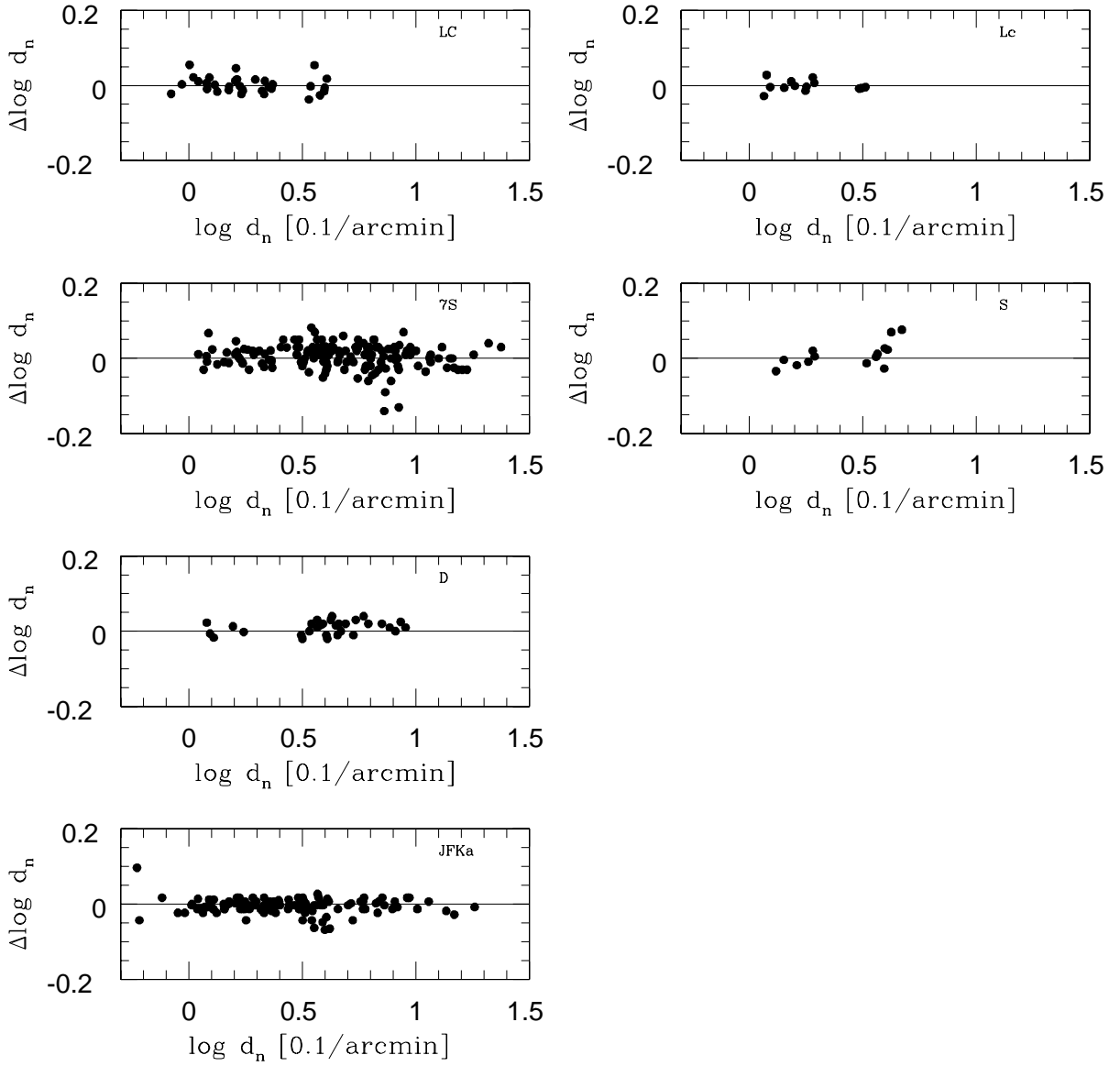


Fig. 7.— Comparison of our measurements of $\log d_n$ with those of other authors. Different panels show this comparison for individual sources: Lucey & Carter (1988) (LC); Faber et al. (1989) (7S); Dressler (1987) and Dressler et al. (1991) (D); Jørgensen et al. (1995a) (JFKa); Lucey et al. (1997) (Lc); and Smith et al. (1997) (S).

Table 1: The cluster sample

Name	α (1950)	δ (1950)	cz_{hel} kms^{-1}	σ_{cl} kms^{-1}	R_p h^{-1} Mpc	N_{gal}		Reference
(1)	(2)	(3)	(4)	(5)	(6)	(7)	(8)	(9)
Northern hemisphere								
7S21	00:18:36	22:00:29	5840	285	-	7	*	S, G
Pisces	01:06:21	32:16:19	5011	358	0.837	24		F, S
HMS0122+3305	01:20:33	33:22:22	4884	540	1.065	11		S
A262	01:50:00	35:56:19	4982	450	1.130	9		F, S, W
A347	02:21:36	41:25:00	5519	768	-	8	*	S, G
Perseus	03:15:18	41:19:58	4967	550	1.110	30		D, F, S
A539	05:13:55	06:24:00	8646	701	-	19	*	JFK
A1367	11:41:41	20:15:25	6486	760	1.043	8		F, HG
Virgo	12:28:02	12:22:55	1101	685	0.846	81		F, HG
Coma	12:56:01	28:07:18	7010	895	1.925	97		D, Da, F, JFK, Lc, S, W
HG50	15:02:35	02:07:39	1707	249	0.451	8		F, HG
A2199	16:25:48	39:37:48	9075	731	1.466	20	*	F, Lc, S, W
Pegasus	23:17:57	08:04:21	3567	405	0.444	5		F
A2634	23:35:45	26:38:39	9318	814	0.917	14	*	F, Lc, S, W
Southern hemisphere								
A194	01:24:37	-01:41:10	5380	408	1.042	21		F, LC, JFKa, JFKb
Fornax	03:34:19	-35:19:27	1433	320	0.781	25		D, F, HG, MDL
Eridanus	03:35:25	-20:38:24	1618	236	0.682	22		HG, Wa
Doradus	03:59:05	-51:16:59	1114	245	1.300	10		HG, JFK, MDL
A3381	06:08:06	-33:34:59	11381	372	-	13	*	JFK
Hydra	10:34:19	-27:26:53	3720	555	0.867	50		F, JFK, LC
AS639	10:38:24	-45:55:59	6246	456	-	10	*	JFK
Cen45	12:46:48	-40:56:19	4650	350	-	10	*	F, HG, LC
Cen30	12:44:12	-40:44:19	3030	658	1.385	36		Db, F, HG, LC
AS714	12:48:17	-26:17:27	3258	215	0.450	8		A
Klemola27	13:46:11	-30:22:03	4611	382	0.670	18		Db, JFK, Wb
AS753	13:58:31	-33:40:08	4167	401	0.979	27		Db, JFK, Wb
PavoII	18:43:49	-63:28:48	4286	284	-	17		F, HG, LC
Klemola44	23:44:52	-28:22:17	8457	375	1.034	32		F, JFK, LC

Notes. — Asterisks in column (8) denote clusters that were not observed by us; data for these clusters come entirely from other authors.

References. — A: Abell et al. (1989); D: Dressler et al. (1987); Da: Dressler (1987); Db: Dressler et al. (1991); F: Faber et al. (1989); G: Gibbons et al. (2000); HG: groups from Huchra & Geller. (1982); JFK: Jørgensen et al. (1996); LC: Lucey & Carter (1988); Lc: Lucey et al. (1997); MDL: groups from Maia et al. (1989); S: Smith et al. (1997); W: Wegner et al. (1999); Wa: Willmer et al. (1989); and Wb: Willmer et al. (1991).

Table 2: Galaxies excluded by our cluster membership assignment

Galaxy	α (1950)	δ (1950)	cz_{hel} kms^{-1}	m_B mag	Cluster	R_p h^{-1} Mpc	σ_{cl} kms^{-1}	R_{proj} h^{-1} Mpc	$ \Delta_{\text{cz}} $ kms^{-1}	References
(1)	(2)	(3)	(4)	(5)	(6)	(7)	(8)	(9)	(10)	(11)
CGCG 385-091	01:20:39	-00:54:11	8269	14.82	A194	1.042	408	1.188	2889	JFKa
NGC 0533	01:22:57	01:29:57	5544	13.44	A194	1.042	408	3.018	164	JFKa
UGC 01269	01:46:11	34:44:05	3848	15.43	A262	1.130	450	11.340	1134	S
UGC 01837	02:19:49	42:47:06	6582	14.63	A347	1.000	768	1.357	1063	S
UGC 01841	02:20:02	42:45:55	6373	14.29	A347	1.000	768	1.328	854	S
PER 195	03:15:48	40:54:04	8342	14.20	Perseus	1.110	550	0.382	3375	D, S
NGC 1705	04:53:06	-53:26:30	597	13.06	Doradus	1.300	245	1.653	517	MDL
[WFC91] 101	13:51:06	-29:34:59	6923	14.75	Klemola27	0.670	382	1.067	2312	W
[WFC91] 039	13:59:18	-32:55:44	10630	15.47	AS753	0.979	401	0.220	6463	JFKa, W
[WFC91] 056	14:00:18	-33:46:56	2718	14.37	AS753	0.979	401	0.282	1449	JFKa, W
ESO 384G037	14:00:38	-33:50:02	5723	14.78	AS753	0.979	401	0.345	1556	JFKa, W
D69	23:44:37	-28:17:42	10071	16.88	Klemola44	1.034	375	0.134	1614	JFKa, LC
D82	23:45:20	-28:13:54	10688	17.12	Klemola44	1.034	375	0.261	2231	LC
D39	23:45:43	-28:27:24	10554	16.30	Klemola44	1.034	375	0.305	2097	JFKa, LC
D65	23:45:47	-28:21:10	10230	15.00	Klemola44	1.034	375	0.298	1773	JFKa, LC

References. — D: Dressler et al. (1987); JFKa: Jørgensen et al. (1995a); LC: Lucey & Carter (1988); MDL: groups from Maia et al. (1989); S: Smith et al. (1997); and W: Willmer et al. (1991).

Table 3: External comparisons of spectroscopic parameters

Sources (1)	N_c (2)	$\Delta \log \sigma$ (3)	$\sigma_{\Delta \log \sigma}$ (4)	N_c (5)	ΔMg_2 (6)	$\sigma_{\Delta \text{Mg}_2}$ (7)
LC	29	0.012 ± 0.011	0.054	–	–	–
7S	115	0.019 ± 0.005	0.055	82	0.004 ± 0.002	0.021
D	25	0.025 ± 0.012	0.055	23	0.005 ± 0.005	0.023
JFKb	64	0.021 ± 0.008	0.059	39	0.004 ± 0.004	0.023
Lc	7	0.009 ± 0.011	0.030	7	0.003 ± 0.006	0.019
S	8	0.011 ± 0.014	0.043	5	0.002 ± 0.007	0.021

References. — As in Table 4.

Table 4: Spectroscopy: sources of the cluster sample

Source	N_σ (meas)	N_σ (gal)	N_σ (sing)	$N_{M_{g_2}}$ (meas)	$N_{M_{g_2}}$ (gal)	$N_{M_{g_2}}$ (sing)
(1)	(2)	(3)	(4)	(5)	(6)	(7)
Our	338	229	91	333	225	105
LC		89	44		—	—
7S		208	58		155	64
D		81	31		53	26
JFKb		157	75		129	91
Lc		85	1		65	45
S		110	65		98	71

References. — JFKb: Jørgensen et al. (1995b); other references are as in Table 1.

Table 5: External comparisons of photometric parameters

Sources (1)	N_c (2)	$\Delta \log d_n$ (3)	$\sigma_{\log d_n}$ (4)
LC	35	0.005 ± 0.004	0.023
7S	162	0.006 ± 0.002	0.024
D	31	0.010 ± 0.003	0.016
JFKa	124	-0.004 ± 0.002	0.013
Lc	13	-0.007 ± 0.004	0.016
S	14	-0.001 ± 0.005	0.019

References. — As in Table 6.

Table 6: Photometry: sources of the cluster sample

Source	Filter	N_{d_n} (meas)	N_{d_n} (gal)	N_{d_n} (sing)
(1)	(2)	(3)	(4)	(5)
Our	R	508	348	117
LC	V		77	19
7S	B		199	42
D	B		63	9
JFKa	Gunn-r		197	59
Lc	V		86	0
S	R		113	65

References. — JFKa: Jørgensen et al. (1995a); other references are as in Table 4.

Table 7. The cluster sample: galaxies entering the $D_n - \sigma$ relation

Name	α	δ	T	m_B	N_s^o	N_s^l	cz_{hel}	$\epsilon_{cz_{hel}}$	$\log \sigma$	$\epsilon_{\log \sigma}$	N_M^o	N_M^l	M_{G2}	$\epsilon_{M_{G2}}$	N_d^o	N_d^l	$\log d_n$	$\epsilon_{\log d_n}$
(1)	(2)	(3)	(4)	(5)	(6)	(7)	(8)	(9)	(10)	(11)	(12)	(13)	(14)	(15)	(16)	(17)	(18)	(19)
7S21																		
CGCG 457-008	00:18:16	+21:15:33	-2	15.18	0	1	5926	60	2.053	0.030	0	1	0.259	0.009	0	1	0.277	0.025
NGC 0079	00:18:27	+22:17:21	-5	14.80	0	1	5479	56	2.280	0.030	0	1	0.312	0.009	0	1	0.354	0.025
NGC 0080	00:18:35	+22:04:49	-3	13.74	0	2	5698	45	2.431	0.015	0	1	0.308	0.010	0	1	0.584	0.011
(SLH97) S06	00:18:45	+21:42:22	-2	15.99	0	1	5646	58	2.103	0.021	0	1	0.211	0.009	0	1	0.018	0.025
NGC 0083	00:18:48	+22:09:00	-5	14.21	0	2	6304	50	2.407	0.014	0	1	0.326	0.009	0	1	0.538	0.011
NGC 0085A	00:18:49	+22:14:04	-2	15.27	0	1	6189	62	2.025	0.030	0	1	0.244	0.009	0	1	0.175	0.025
IC 1548	00:19:19	+21:43:45	-2	15.15	0	1	5775	59	2.165	0.030	0	1	0.202	0.009	0	1	0.294	0.025
Pisces																		
(SLH97) Z17005	00:56:43	+32:52:04	-5	15.58	0	1	4651	50	2.010	0.030	0	1	0.208	0.009	0	1	0.191	0.025
CGCG 501-070	00:59:25	+32:11:00	-5	14.89	0	1	4263	47	2.294	0.024	0	1	0.327	0.007	0	1	0.365	0.025
CGCG 501-077	01:02:49	+32:09:44	-5	15.30	0	1	5156	54	2.079	0.024	0	1	0.270	0.007	0	1	0.248	0.025
IC 1618	01:03:11	+32:08:41	-2	15.44	0	1	4730	50	1.948	0.040	0	1	0.226	0.012	0	1	0.187	0.025
NGC 0375	01:04:20	+32:04:52	-2	15.38	0	1	5920	60	2.249	0.040	0	1	0.277	0.012	0	1	0.257	0.025
NGC 0379	01:04:30	+32:15:16	-3	14.16	0	1	5556	44	2.375	0.015	0	1	0.308	0.008	0	1	0.569	0.011
NGC 0383	01:04:39	+32:08:46	-3	13.59	0	1	5071	40	2.445	0.016	0	1	0.313	0.002	0	1	0.705	0.011
NGC 0384	01:04:39	+32:01:32	-5	14.35	0	1	4266	47	2.410	0.021	0	1	0.314	0.006	0	1	0.504	0.025
NGC 0385	01:04:42	+32:03:10	-3	14.38	0	1	5024	40	2.286	0.016	0	1	0.293	0.002	0	1	0.477	0.011
NGC 0388	01:05:01	+32:02:36	-5	15.33	0	1	5464	56	2.130	0.024	0	1	0.257	0.007	0	1	0.261	0.025
(SLH97) Z01032	01:05:27	+32:11:13	-2	15.89	0	1	4763	51	2.011	0.040	0	1	0.274	0.012	0	1	0.074	0.025
NGC 0392	01:05:36	+32:52:00	-3	13.90	0	1	4672	37	2.394	0.017	0	1	0.302	0.008	0	1	0.571	0.011
NGC 0394	01:05:40	+32:52:53	-2	14.74	0	1	4388	48	2.257	0.021	0	1	0.270	0.006	0	1	0.406	0.025
NGC 0397	01:05:45	+32:50:34	-5	15.46	0	1	4988	52	2.083	0.030	0	1	0.261	0.009	0	1	0.222	0.025
NGC 0398	01:06:08	+32:14:53	-2	15.21	0	1	4912	52	2.006	0.030	0	1	0.264	0.009	0	1	0.268	0.025
CGCG 501-102	01:06:27	+31:42:48	-5	15.19	0	1	5176	54	2.187	0.024	0	1	0.280	0.007	0	1	0.284	0.025
NGC 0410	01:08:12	+32:53:12	-5	12.60	0	1	5294	42	2.487	0.014	0	1	0.346	0.006	0	1	0.744	0.011
CGCG 501-126	01:09:05	+31:17:38	-2	15.73	0	1	4852	51	1.919	0.030	0	1	0.230	0.009	0	1	0.101	0.025
NGC 0420	01:09:23	+31:51:29	-2	13.40	1	1	4940	11	2.289	0.023	1	1	0.250	0.002	1	1	0.559	0.005
IC 1638	01:09:35	+33:05:58	-2	14.91	0	1	4828	51	2.153	0.016	0	1	0.278	0.005	0	1	0.341	0.025
IC 1648	01:10:55	+32:57:13	-2	15.18	0	1	5541	57	2.083	0.030	0	1	0.269	0.009	0	1	0.272	0.025
HMS0122+33																		
IC 1673	01:17:58	+32:46:59	-5	14.92	0	1	5090	53	2.268	0.030	0	1	0.277	0.009	0	1	0.361	0.025
CGCG 502-043	01:18:17	+33:07:02	-5	15.19	0	1	5237	54	2.097	0.024	0	1	0.268	0.009	0	1	0.270	0.025
IC 1680	01:18:58	+33:01:27	-2	15.14	0	1	4438	48	2.122	0.030	0	1	0.269	0.009	0	1	0.295	0.025
NGC 0499	01:20:22	+33:11:59	-2	13.00	0	1	4375	35	2.400	0.018	0	1	0.334	0.005	0	1	0.701	0.011
NGC 0501	01:20:36	+33:10:20	-5	15.64	0	1	4887	41	2.214	0.019	0	1	0.308	0.002	0	1	0.261	0.011
NGC 0504	01:20:42	+32:57:00	-2	14.00	1	0	4226	43	2.471	0.030	1	0	0.311	0.009	1	0	0.730	0.007
NGC 0507	01:20:50	+32:59:42	-3	11.89	0	1	4917	41	2.498	0.014	0	1	0.303	0.003	0	1	0.732	0.011
NGC 0517	01:21:54	+33:10:09	-2	13.60	2	0	4202	19	2.340	0.018	2	0	0.279	0.005	1	0	0.560	0.005
NGC 0528	01:22:42	+33:24:43	-2	13.70	1	1	4807	72	2.381	0.021	1	0	0.306	0.008	1	1	0.566	0.005
NGC 0529	01:22:54	+34:28:00	-3	13.10	2	0	4820	22	2.388	0.017	2	0	0.305	0.002	1	0	0.700	0.012
A262																		
NGC 0679	01:46:48	+35:32:00	-3	13.10	0	1	5054	40	2.408	0.018	0	1	0.304	0.011	0	1	0.630	0.011
NGC 0687	01:47:36	+36:07:00	-2	13.30	0	1	5147	41	2.352	0.017	0	1	0.301	0.012	0	1	0.640	0.011
CGCG 522-033	01:49:36	+35:52:08	-5	15.66	0	1	4284	47	2.094	0.024	0	1	0.272	0.007	0	1	0.153	0.025
NGC 0708	01:49:50	+35:54:20	-5	12.36	2	1	4827	40	2.372	0.022	0	1	0.321	0.011	0	1	0.502	0.011
CGCG 522-046	01:50:24	+36:43:00	-3	14.40	1	0	5296	60	2.308	0.028	1	0	0.285	0.008	1	0	0.480	0.010
IC 0171	01:52:18	+35:02:00	-5	13.23	0	1	5362	42	2.270	0.026	0	0	0.000	0.000	1	0	0.650	0.005
NGC 0759	01:54:54	+36:05:58	-5	13.70	0	1	4714	37	2.430	0.017	0	1	0.266	0.011	2	1	0.605	0.010

Table 7—Continued

Name	α	δ	T	m_B	N_s^o	N_s^l	cz_{hel}	$\epsilon_{cz_{hel}}$	$\log \sigma$	$\epsilon_{\log \sigma}$	N_M^o	N_M^l	Mg2	ϵ_{Mg2}	N_d^o	N_d^l	$\log d_n$	$\epsilon_{\log d_n}$	
(1)	(1950)	(1950)	(4)	(5)	(6)	(7)	(8)	(9)	(10)	(11)	(12)	(13)	(14)	(15)	(16)	(17)	(18)	(19)	
CGCG 522-089	01:55:02	+36:40:29	-5	15.70	0	1	5245	54	1.953	0.030	0	1	0.222	0.009	0	1	0.119	0.025	
A347																			
CGCG 538-065	02:21:43	+43:05:57	-2	14.77	0	1	5301	55	2.308	0.030	0	1	0.314	0.009	0	1	0.425	0.025	
NGC 0909	02:22:14	+41:48:37	-5	14.50	1	1	4965	66	2.268	0.018	1	1	0.281	0.005	1	1	0.472	0.008	
NGC 0910	02:22:18	+41:36:00	-5	14.50	1	0	5207	21	2.387	0.025	1	0	0.341	0.011	1	0	0.610	0.012	
NGC 0911	02:22:33	+41:43:51	-2	14.32	1	1	5766	59	2.400	0.030	0	1	0.328	0.009	0	1	0.534	0.025	
NGC 0912	02:22:34	+41:33:08	-5	14.92	0	1	4418	48	2.235	0.030	0	1	0.295	0.009	0	1	0.360	0.025	
NGC 0946	02:27:30	+42:01:00	-2	14.50	2	0	5772	20	2.295	0.022	2	0	0.248	0.002	1	0	0.530	0.010	
CGCG 539-042	02:29:18	+41:43:27	-5	14.99	0	1	4885	52	2.185	0.030	0	1	0.272	0.009	0	1	0.342	0.025	
Perseus																			
CGCG 540-046	03:06:00	+42:47:00	-2	14.50	2	0	5659	14	2.337	0.017	2	0	0.277	0.001	1	0	0.630	0.009	
IC 0293	03:07:40	+40:56:54	-5	15.04	0	1	4714	50	2.171	0.040	0	1	0.274	0.012	0	1	0.336	0.025	
NGC 1224	03:07:57	+41:10:31	-2	14.45	0	1	5235	54	2.384	0.030	0	1	0.274	0.009	0	1	0.544	0.025	
IC 0310	03:13:24	+41:08:00	-2	13.12	2	1	5678	10	2.352	0.013	2	1	0.284	0.011	1	1	0.612	0.008	
IC 0312	03:14:50	+41:34:19	-2	14.60	0	1	4988	52	2.342	0.040	0	1	0.310	0.012	0	1	0.532	0.025	
PGC 012292	03:15:00	+41:17:00	-5	15.80	0	1	3544	41	2.081	0.030	0	1	0.243	0.009	0	1	0.134	0.025	
CGCG 540-087	03:15:06	+41:14:00	-5	14.81	0	1	6461	64	2.294	0.021	0	1	0.269	0.006	0	1	0.456	0.025	
PGC 012349	03:15:39	+41:31:18	-5	15.36	0	1	4247	46	2.192	0.030	0	1	0.279	0.009	0	1	0.294	0.025	
PGC 012378	03:16:00	+41:28:00	-5	15.23	0	1	6213	62	2.317	0.003	0	1	0.292	0.009	0	1	0.362	0.025	
NGC 1272	03:16:06	+41:18:35	-3	14.50	2	1	3740	24	2.461	0.011	1	1	0.336	0.006	1	1	0.685	0.025	
NGC 1273	03:16:08	+41:21:34	-2	13.78	0	1	5354	44	2.332	0.020	0	1	0.279	0.011	0	1	0.582	0.011	
IC 1907	03:16:16	+41:23:58	-2	14.77	0	1	4489	48	2.285	0.040	0	1	0.292	0.012	0	1	0.468	0.025	
NGC 1274	03:16:21	+41:22:00	-5	15.10	1	1	6395	52	2.291	0.022	0	1	0.300	0.008	0	1	0.480	0.011	
PGC 012423	03:16:26	+41:16:00	-5	16.52	0	1	3963	44	1.925	0.030	0	1	0.283	0.009	0	1	0.023	0.025	
NGC 1278	03:16:35	+41:22:59	-5	14.40	0	2	6090	41	2.423	0.013	0	1	0.314	0.005	0	1	0.655	0.011	
CGCG 540-107	03:16:43	+41:04:15	-5	14.79	0	1	4434	48	2.290	0.040	0	1	0.302	0.012	0	1	0.457	0.025	
NGC 1281	03:16:47	+41:26:58	-5	14.66	0	1	4300	47	2.432	0.030	0	1	0.328	0.009	0	1	0.503	0.025	
NGC 1282	03:16:53	+41:11:12	-5	14.30	0	1	2139	40	2.345	0.017	0	1	0.277	0.011	1	1	0.637	0.023	
NGC 1283	03:16:57	+41:13:06	-5	14.01	0	1	6727	55	2.343	0.019	0	1	0.302	0.010	0	1	0.470	0.011	
PGC 012544	03:17:31	+41:11:30	-2	15.14	0	1	4950	52	2.216	0.030	0	1	0.293	0.009	0	1	0.394	0.025	
IC 0313	03:17:39	+41:42:50	-2	15.05	0	1	4432	48	2.375	0.030	0	1	0.335	0.009	0	1	0.507	0.025	
NGC 1293	03:18:18	+41:12:50	-5	13.67	0	1	4132	35	2.350	0.019	0	1	0.334	0.011	0	1	0.550	0.011	
CGCG 540-119	03:18:45	+40:41:08	-5	14.31	0	1	6421	46	2.557	0.024	0	1	0.340	0.007	0	1	0.620	0.025	
CGCG 540-123	03:21:18	+40:30:53	-5	15.06	0	1	3793	43	2.189	0.024	0	1	0.239	0.007	0	1	0.528	0.025	
CGCG 541-004	03:22:10	+41:03:56	-2	14.88	0	1	6215	62	2.333	0.030	0	1	0.297	0.009	0	1	0.482	0.025	
CGCG 525-043	03:31:00	+39:22:44	-2	14.30	2	0	6104	17	2.322	0.017	2	0	0.275	0.004	1	0	0.620	0.008	
A539																			
0512+0612	05:12:55	+06:12:32	-2	17.16	0	1	8742	70	2.199	0.019	0	1	0.242	0.010	2	1	0.205	0.005	
0513+0616	05:13:07	+06:16:02	-2	17.19	0	1	8634	70	2.224	0.030	0	1	0.263	0.010	2	1	0.235	0.005	
CGCG 421-015	05:13:33	+06:23:34	-2	17.10	0	1	6664	54	2.377	0.018	0	1	0.257	0.012	2	1	0.337	0.005	
0513+0617	05:13:44	+06:17:18	-2	16.80	0	1	8708	69	2.350	0.025	0	1	0.316	0.008	1	1	0.271	0.005	
CGCG 421-016	05:13:49	+06:20:54	-2	17.20	0	1	7429	60	2.291	0.018	0	1	0.273	0.012	2	1	0.291	0.005	
CGCG 421-017	05:13:54	+06:26:59	-5	17.45	0	1	7101	56	2.254	0.029	0	1	0.236	0.010	1	1	0.314	0.005	
MCG +01-14-014	05:13:55	+06:26:05	-2	17.80	0	1	9292	74	2.274	0.022	0	1	0.280	0.011	3	1	0.246	0.005	
MCG +01-14-018	05:13:57	+06:27:28	-2	17.90	0	1	7879	63	2.152	0.027	0	1	0.269	0.009	1	1	0.034	0.005	
0513+0624	05:13:58	+06:24:37	-2	17.25	0	1	9363	75	2.220	0.023	0	1	0.263	0.011	3	1	0.173	0.005	
0514+0628	05:14:03	+06:28:55	-2	17.90	0	1	9931	79	2.378	0.028	0	1	0.304	0.009	1	1	0.134	0.005	
0514+0619a	05:14:05	+06:19:29	-2	17.20	0	1	8410	67	2.087	0.034	0	1	0.199	0.011	1	1	-0.022	0.015	
0514+0619b	05:14:10	+06:19:34	-2	17.30	0	1	8129	65	2.198	0.031	0	1	0.262	0.010	1	1	0.104	0.005	

Table 7—Continued

Name	α	δ	T	m_B	N_s^o	N_s^l	$c_{z_{hel}}$	$\epsilon_{c_{z_{hel}}}$	$\log \sigma$	$\epsilon_{\log \sigma}$	N_M^o	N_M^l	Mg2	ϵ_{Mg2}	N_d^o	N_d^l	$\log d_n$	$\epsilon_{\log d_n}$
(1)	(2)	(3)	(4)	(5)	(6)	(7)	(8)	(9)	(10)	(11)	(12)	(13)	(14)	(15)	(16)	(17)	(18)	(19)
0514+0620	05:14:08	+06:20:06	-2	16.70	0	1	8677	69	2.172	0.034	0	1	0.265	0.011	1	1	0.118	0.008
CGCG 421-019	05:14:14	+06:29:56	-5	16.19	0	1	9699	78	2.511	0.022	0	1	0.338	0.011	2	1	0.461	0.005
A1367																		
NGC 3805	11:38:12	+20:37:00	-3	13.80	1	0	6592	60	2.464	0.018	1	0	0.326	0.010	1	0	0.580	0.006
NGC 3841	11:41:26	+20:14:57	-5	14.95	0	1	6363	52	2.338	0.028	0	1	0.309	0.009	0	1	0.280	0.011
NGC 3842	11:41:26	+20:13:39	-5	13.30	0	2	6237	49	2.501	0.015	0	1	0.337	0.011	0	1	0.530	0.011
NGC 3862	11:42:29	+19:53:02	-5	14.00	0	2	6462	51	2.429	0.021	0	1	0.296	0.009	1	1	0.493	0.017
NGC 3873	11:43:10	+20:03:06	-5	14.20	0	2	5438	43	2.398	0.022	0	1	0.300	0.008	0	1	0.450	0.011
NGC 3886	11:44:30	+20:07:00	-3	14.30	1	0	5842	75	2.416	0.027	1	0	0.321	0.010	2	0	0.535	0.009
Virgo																		
NGC 4168	12:09:44	+13:29:00	-5	12.77	0	2	2307	18	2.271	0.018	0	1	0.000	0.000	0	1	0.740	0.011
NGC 4179	12:10:18	+01:35:00	-2	12.21	0	1	1239	24	2.215	0.040	0	1	0.000	0.000	1	0	0.960	0.008
NGC 4239	12:14:42	+16:48:00	-5	13.50	1	1	926	20	1.799	0.042	1	1	0.172	0.011	1	1	0.470	0.010
NGC 4255	12:16:24	+05:03:49	-2	13.50	2	0	1981	13	2.176	0.021	2	0	0.272	0.005	1	0	0.640	0.008
NGC 4262	12:17:00	+15:09:00	-3	12.67	0	1	1376	11	2.253	0.053	0	1	0.000	0.000	1	0	0.890	0.018
NGC 4267	12:17:12	+13:05:00	-3	12.17	0	1	1001	23	2.217	0.029	0	1	0.000	0.000	1	0	0.900	0.009
NGC 4270	12:17:18	+05:44:00	-2	13.26	1	0	2364	17	2.140	0.066	1	0	0.207	0.011	1	0	0.690	0.005
NGC 4318	12:20:12	+08:29:00	-5	14.40	1	1	1244	29	1.978	0.020	1	0	0.213	0.011	1	1	0.490	0.005
NGC 4339	12:21:00	+06:22:00	-5	12.83	1	1	1305	22	2.031	0.021	1	1	0.257	0.004	2	1	0.737	0.005
NGC 4350	12:21:24	+16:58:00	-2	12.30	0	1	1247	24	2.297	0.020	0	0	0.000	0.000	2	0	0.980	0.006
NGC 4365	12:21:55	+07:35:40	-5	11.18	0	2	1240	24	2.416	0.012	0	1	0.321	0.012	0	1	1.100	0.011
NGC 4374	12:22:30	+13:10:00	-5	10.82	2	2	1022	12	2.473	0.010	2	1	0.306	0.002	1	1	1.257	0.005
NGC 4377	12:22:40	+15:02:24	-3	13.20	0	1	1375	11	2.143	0.053	0	0	0.000	0.000	3	0	0.800	0.006
NGC 4379	12:22:42	+15:53:00	-3	12.77	2	1	1064	21	2.012	0.020	2	0	0.234	0.005	1	0	0.780	0.009
NGC 4382	12:22:54	+18:28:00	-2	10.43	0	1	758	21	2.312	0.016	0	0	0.000	0.000	1	0	1.250	0.007
NGC 4387	12:23:12	+13:05:15	-5	13.42	1	1	567	16	1.997	0.018	1	1	0.251	0.010	1	1	0.700	0.011
NGC 4406	12:23:42	+13:13:00	-5	10.75	0	2	-221	16	2.390	0.019	0	0	0.000	0.000	1	1	1.220	0.010
NGC 4415	12:24:08	+08:42:42	-5	14.20	3	0	933	19	1.676	0.049	3	0	0.131	0.009	1	0	0.170	0.005
NGC 4417	12:24:18	+09:51:42	-2	12.43	2	1	830	21	2.096	0.015	2	0	0.257	0.005	1	0	0.900	0.010
NGC 4434	12:25:00	+08:26:00	-5	13.20	0	1	1068	23	2.077	0.023	0	1	0.264	0.010	0	1	0.680	0.011
NGC 4442	12:25:30	+10:05:00	-2	11.70	0	1	515	19	2.294	0.033	0	0	0.000	0.000	1	0	1.070	0.010
NGC 4458	12:26:25	+13:31:06	-5	13.32	0	1	662	15	2.041	0.030	0	1	0.219	0.010	1	1	0.618	0.005
NGC 4461	12:26:31	+13:27:42	-2	12.37	0	1	1925	15	2.228	0.039	0	0	0.000	0.000	2	0	0.895	0.005
NGC 4472	12:27:14	+08:16:36	-5	9.84	2	1	977	19	2.488	0.013	2	1	0.316	0.005	2	1	1.386	0.005
NGC 4473	12:27:18	+13:42:00	-5	11.61	0	2	2236	17	2.276	0.024	0	0	0.000	0.000	0	1	1.090	0.011
NGC 4474	12:27:22	+14:20:42	-2	12.95	1	0	1639	15	1.968	0.033	1	0	0.245	0.011	1	0	0.780	0.006
NGC 4477	12:27:31	+13:54:42	-2	11.62	0	1	1355	10	2.310	0.023	0	0	0.000	0.000	1	0	1.010	0.008
NGC 4478	12:27:46	+12:36:18	-5	12.57	0	2	1370	10	2.168	0.018	0	1	0.254	0.009	0	1	0.920	0.011
NGC 4479	12:27:46	+13:51:12	-2	13.93	1	0	869	47	1.915	0.038	1	0	0.155	0.011	1	0	0.420	0.009
NGC 4489	12:28:18	+17:02:00	-5	13.20	1	1	982	22	1.720	0.047	1	1	0.187	0.011	1	1	0.573	0.005
NGC 4515	12:30:30	+16:32:00	-3	13.30	1	0	951	11	1.902	0.035	1	0	0.204	0.011	1	0	0.570	0.006
NGC 4528	12:31:34	+11:35:48	-3	12.98	0	1	1374	10	2.049	0.034	0	0	0.000	0.000	1	0	0.780	0.007
NGC 4550	12:33:00	+12:30:00	-2	12.73	1	1	437	56	1.967	0.022	1	0	0.172	0.011	1	0	0.850	0.013
NGC 4551	12:33:06	+12:32:00	-5	13.27	2	1	1198	24	2.007	0.020	2	1	0.244	0.011	1	1	0.740	0.010
NGC 4564	12:33:55	+11:42:54	-5	12.24	0	1	1165	24	2.196	0.025	0	1	0.318	0.008	0	1	0.900	0.011
NGC 4570	12:34:24	+07:31:00	-2	12.24	0	1	1730	13	2.255	0.043	0	0	0.000	0.000	1	0	0.990	0.010
NGC 4578	12:35:00	+09:50:00	-2	12.48	0	1	2284	18	2.185	0.043	0	0	0.000	0.000	1	0	0.750	0.007
NGC 4600	12:37:48	+03:24:00	-2	13.70	1	0	852	65	1.867	0.035	1	0	0.139	0.011	1	0	0.470	0.007
NGC 4621	12:39:30	+11:55:00	-5	11.28	0	1	444	18	2.367	0.013	0	1	0.326	0.009	0	1	1.130	0.011

Table 7—Continued

Name	α	δ	T	m_B	N_s^o	N_s^l	$c_{z_{hel}}$	$\epsilon_{c_{z_{hel}}}$	$\log \sigma$	$\epsilon_{\log \sigma}$	N_M^o	N_M^l	Mg ₂	ϵ_{Mg_2}	N_d^o	N_d^l	$\log d_n$	$\epsilon_{\log d_n}$
(1)	(2)	(3)	(4)	(5)	(6)	(7)	(8)	(9)	(10)	(11)	(12)	(13)	(14)	(15)	(16)	(17)	(18)	(19)
NGC 4636	12:40:18	+02:58:00	-5	11.01	0	1	937	22	2.318	0.017	0	1	0.312	0.009	0	1	1.080	0.011
NGC 4649	12:41:06	+11:49:00	-5	10.30	0	1	1095	23	2.540	0.011	0	1	0.340	0.009	0	1	1.300	0.011
NGC 4660	12:42:00	+11:28:00	-5	12.30	0	1	1115	23	2.307	0.011	0	1	0.297	0.010	0	1	0.910	0.011
NGC 4733	12:48:36	+11:11:00	-3	13.20	2	1	928	19	1.818	0.041	2	1	0.191	0.008	0	1	0.580	0.011
Coma																		
IC 3618	12:36:48	+26:57:19	-5	15.13	0	1	6623	52	2.291	0.024	0	0	0.000	0.000	0	1	0.247	0.011
CGCG 159-043	12:36:51	+28:02:51	-5	15.05	0	1	6710	53	2.415	0.028	0	0	0.000	0.000	0	1	0.340	0.011
IC 3623	12:37:00	+27:22:28	-5	15.10	0	1	7068	56	2.231	0.030	0	0	0.000	0.000	0	1	0.308	0.011
CGCG 169-063	12:41:25	+27:08:11	-5	15.70	0	1	7566	60	2.184	0.025	0	1	0.000	0.000	0	1	0.173	0.011
NGC 4673	12:43:06	+27:20:00	-5	13.70	0	1	6939	55	2.360	0.023	0	1	0.000	0.000	0	1	0.578	0.011
NGC 4692	12:45:28	+27:29:39	-5	13.95	0	2	7996	65	2.408	0.019	0	1	0.315	0.009	0	2	0.482	0.032
CGCG 159-083	12:47:16	+27:09:37	-5	15.60	0	1	6887	56	2.320	0.030	0	0	0.000	0.000	0	1	0.374	0.011
CGCG 159-089	12:48:28	+28:06:54	-5	15.80	0	1	7606	60	2.242	0.032	0	0	0.000	0.000	0	1	0.297	0.011
IC 0832	12:51:33	+26:42:46	-5	16.17	0	1	7094	57	2.334	0.029	0	1	0.000	0.000	0	1	0.303	0.011
NGC 4807	12:53:06	+27:47:00	-3	14.40	0	2	6941	55	2.329	0.017	0	1	0.283	0.012	0	2	0.410	0.021
IC 3900	12:53:16	+27:31:15	-2	15.93	0	1	7115	57	2.445	0.029	0	1	0.000	0.000	0	1	0.374	0.011
NGC 4816	12:53:48	+28:01:00	-3	14.10	0	3	6878	55	2.351	0.014	0	2	0.311	0.002	0	3	0.390	0.011
IC 0834	12:53:53	+26:37:40	-5	15.98	0	1	6457	52	2.429	0.024	0	1	0.000	0.000	0	1	0.350	0.011
CGCG 160-023	12:53:54	+28:01:16	-5	16.47	0	1	6903	56	2.263	0.023	0	0	0.000	0.000	0	1	0.233	0.011
CGCG 160-027	12:54:01	+28:06:03	-5	16.53	0	2	6275	51	2.240	0.021	0	1	0.282	0.008	0	2	0.193	0.011
NGC 4824	12:54:09	+27:48:33	-5	16.77	0	2	7117	57	2.209	0.020	0	1	0.278	0.010	0	2	0.149	0.011
NGC 4827	12:54:18	+27:26:55	-5	15.51	0	1	7599	61	2.442	0.023	0	0	0.000	0.000	0	1	0.458	0.011
CGCG 160-037	12:54:44	+27:44:11	-5	16.33	0	1	7480	60	2.372	0.024	0	0	0.000	0.000	0	1	0.292	0.011
NGC 4839	12:54:59	+27:46:00	-3	13.60	0	4	7335	58	2.444	0.011	0	2	0.314	0.001	1	4	0.492	0.005
NGC 4840	12:55:07	+27:52:48	-2	15.83	0	2	6097	49	2.390	0.016	0	0	0.000	0.000	0	2	0.386	0.011
CGCG 160-049	12:55:24	+28:27:01	-2	16.69	0	2	7245	58	2.245	0.020	0	1	0.270	0.010	0	2	0.181	0.011
NGC 4850	12:55:57	+28:14:16	-2	16.19	0	2	6039	49	2.247	0.020	0	1	0.268	0.009	0	2	0.280	0.011
CGCG 160-065	12:56:05	+28:17:04	-5	15.23	0	2	7191	58	2.264	0.020	0	1	0.301	0.009	0	2	0.286	0.011
NGC 4854	12:56:22	+27:56:40	-2	15.05	0	2	8430	66	2.268	0.018	0	2	0.316	0.003	0	2	0.199	0.011
IC 3947	12:56:27	+28:03:16	-5	16.68	0	2	5677	46	2.162	0.019	0	1	0.277	0.010	0	2	0.184	0.011
PGC 044522	12:56:31	+28:14:12	-2	16.50	0	2	5652	45	2.199	0.017	0	2	0.279	0.007	0	4	0.084	0.011
PGC 044533	12:56:36	+28:14:23	-2	16.70	0	1	8311	66	1.925	0.035	0	0	0.000	0.000	0	1	-0.157	0.015
NGC 4860	12:56:39	+28:23:36	-5	14.69	0	3	7948	65	2.414	0.012	0	1	0.337	0.007	0	3	0.420	0.011
1256+2820	12:56:40	+28:19:11	-2	17.15	0	1	5071	40	2.091	0.034	0	0	0.000	0.000	0	1	-0.029	0.011
IC 3955	12:56:41	+28:16:06	-2	16.51	0	2	7715	62	2.269	0.020	0	2	0.296	0.004	0	2	0.199	0.011
IC 3957	12:56:43	+28:02:21	-5	15.60	0	2	6350	50	2.185	0.023	0	2	0.292	0.002	1	3	0.152	0.005
IC 3959	12:56:43	+28:03:12	-5	15.20	0	4	7121	25	2.298	0.012	0	2	0.307	0.002	1	4	0.288	0.005
IC 3960	12:56:43	+28:07:27	-2	16.62	1	1	6651	30	2.218	0.020	1	1	0.328	0.002	1	1	0.188	0.005
IC 3963	12:56:49	+28:02:43	-2	16.83	0	2	6675	54	2.120	0.021	0	2	0.266	0.005	0	3	0.111	0.005
PGC 044581	12:56:56	+28:09:25	-5	15.90	0	1	6439	53	1.861	0.043	0	1	0.233	0.011	1	2	-0.063	0.024
NGC 4869	12:56:58	+28:10:54	-5	14.90	0	2	6703	53	2.313	0.015	0	2	0.317	0.002	1	3	0.353	0.030
PGC 044585	12:56:58	+28:10:05	-2	15.00	0	1	5092	40	2.227	0.028	0	0	0.000	0.000	0	2	0.060	0.007
PGC 044596	12:57:00	+28:00:46	-2	17.05	0	2	6033	63	2.175	0.019	0	2	0.273	0.004	1	2	0.081	0.009
PGC 044597	12:57:01	+28:14:23	-2	17.40	0	2	7601	61	2.115	0.021	0	2	0.260	0.005	0	3	-0.045	0.015
PGC 044598	12:57:01	+28:14:42	-2	17.09	0	2	6082	45	2.109	0.021	0	2	0.248	0.005	0	3	0.026	0.005
PGC 044594	12:57:02	+28:16:04	-2	17.80	0	2	6731	53	2.024	0.028	0	1	0.231	0.012	0	2	-0.098	0.011
NGC 4873	12:57:08	+28:15:10	-2	16.34	0	1	5662	46	2.201	0.031	0	1	0.285	0.010	0	2	0.218	0.011
NGC 4874	12:57:11	+28:13:41	-3	14.01	0	3	7176	57	2.418	0.013	0	2	0.322	0.001	1	4	0.513	0.005
NGC 4875	12:57:13	+28:10:36	-2	16.63	0	2	8056	63	2.259	0.017	0	2	0.282	0.005	1	3	0.205	0.005

Table 7—Continued

Name	α	δ	T	m_B	N_s^o	N_s^l	$c_{z_{hel}}$	$\epsilon_{c_{z_{hel}}}$	$\log \sigma$	$\epsilon_{\log \sigma}$	N_M^o	N_M^l	M_{g_2}	$\epsilon_{M_{g_2}}$	N_d^o	N_d^l	$\log d_n$	$\epsilon_{\log d_n}$
(1)	(2)	(3)	(4)	(5)	(6)	(7)	(8)	(9)	(10)	(11)	(12)	(13)	(14)	(15)	(16)	(17)	(18)	(19)
CGCG 160-233	12:57:18	+28:11:47	-5	15.70	0	2	6946	55	2.244	0.014	0	1	0.252	0.010	0	4	0.091	0.005
NGC 4876	12:57:19	+28:10:54	-5	15.10	0	3	6654	53	2.272	0.014	0	1	0.248	0.010	1	3	0.257	0.005
PGC 044656	12:57:19	+28:15:57	-5	16.00	0	2	6652	53	2.139	0.023	0	2	0.280	0.002	1	3	0.059	0.009
IC 3998	12:57:22	+28:14:36	-2	15.60	0	1	9371	74	2.211	0.023	0	0	0.000	0.000	1	3	0.111	0.011
PGC 044679	12:57:30	+28:23:51	-5	16.31	0	2	7544	62	2.087	0.021	0	2	0.264	0.002	0	2	0.040	0.011
NGC 4883	12:57:31	+28:18:24	-2	16.30	0	2	7961	64	2.244	0.022	0	2	0.293	0.004	1	2	0.245	0.005
NGC 4881	12:57:33	+28:30:60	-3	14.85	0	3	6691	53	2.304	0.013	0	1	0.285	0.008	0	4	0.351	0.011
IC 4011	12:57:42	+28:16:18	-5	15.60	0	1	7216	57	2.053	0.020	0	1	0.273	0.006	0	3	0.089	0.005
NGC 4884	12:57:43	+28:14:42	-3	13.17	0	3	6512	52	2.604	0.008	0	2	0.353	0.005	0	4	0.705	0.005
IC 4012	12:57:43	+28:20:48	-5	15.70	0	2	7228	57	2.264	0.017	0	2	0.292	0.002	0	3	0.220	0.011
NGC 4895A	12:57:44	+28:26:31	-5	16.03	0	2	6764	56	2.179	0.023	0	2	0.266	0.002	0	2	0.117	0.011
PGC 044723	12:57:48	+28:20:48	-2	16.10	0	2	7381	59	2.149	0.020	0	2	0.284	0.005	0	3	0.093	0.011
IC 4021	12:57:50	+28:18:30	-2	15.88	0	2	5789	48	2.211	0.020	0	2	0.299	0.002	0	2	0.163	0.011
NGC 4894	12:57:52	+28:14:20	-2	16.98	0	1	4587	37	1.986	0.034	0	1	0.226	0.011	0	2	0.072	0.011
IC 4026	12:57:58	+28:19:04	-2	16.74	0	2	8153	66	2.153	0.022	0	2	0.285	0.004	0	2	0.136	0.011
1258+2747	12:58:02	+27:47:04	-5	17.18	0	2	7815	63	2.015	0.027	0	1	0.260	0.012	0	2	0.010	0.011
PGC 044763	12:58:03	+28:13:38	-2	17.22	0	2	6927	55	2.194	0.021	0	2	0.277	0.005	0	2	0.063	0.011
NGC 4906	12:58:15	+28:11:30	-5	15.20	0	2	7505	60	2.233	0.022	0	2	0.291	0.003	1	3	0.251	0.005
IC 4041	12:58:16	+28:16:06	-2	15.30	0	2	7056	61	2.131	0.023	0	2	0.280	0.005	1	2	0.091	0.005
PGC 044815	12:58:20	+28:22:08	-2	17.31	0	1	6611	53	1.968	0.041	0	1	0.249	0.011	0	1	-0.049	0.011
PGC 044821	12:58:24	+28:11:30	-2	16.40	0	1	8655	50	2.335	0.030	0	0	0.000	0.000	1	2	0.340	0.011
IC 4051	12:58:29	+28:16:36	-3	14.80	0	1	4964	39	2.366	0.021	0	0	0.000	0.000	1	2	0.318	0.007
CGCG 160-092	12:58:45	+28:05:18	-5	17.15	0	2	5972	48	2.194	0.024	0	1	0.265	0.011	0	2	0.026	0.011
NGC 4923	12:59:07	+28:06:57	-5	14.85	0	2	5516	46	2.307	0.016	0	2	0.311	0.005	0	3	0.356	0.011
IC 0843	12:59:10	+29:23:58	-5	15.67	0	1	7397	60	2.404	0.021	0	0	0.000	0.000	0	1	0.392	0.011
CGCG 160-100	12:59:26	+28:09:43	-5	15.93	0	2	7621	60	2.276	0.018	0	1	0.285	0.010	0	2	0.179	0.011
1259+2752	12:59:23	+27:52:21	-2	17.36	1	0	8241	18	1.912	0.035	1	0	0.242	0.011	1	0	-0.120	0.013
NGC 4926	12:59:29	+27:53:36	-3	14.40	0	3	7751	62	2.426	0.011	0	2	0.324	0.002	1	4	0.483	0.005
NGC 4927	12:59:33	+28:16:28	-5	15.78	0	2	7747	62	2.456	0.020	0	1	0.354	0.010	0	2	0.355	0.011
1259+2755	12:59:36	+27:55:17	-2	17.33	1	0	7095	20	2.019	0.051	1	0	0.219	0.009	2	0	-0.065	0.038
IC 4133	13:01:27	+28:15:23	-5	16.53	0	2	6369	51	2.229	0.019	0	1	0.289	0.010	0	2	0.236	0.011
NGC 4952	13:02:35	+29:23:24	-5	13.60	0	1	5865	46	2.439	0.018	0	0	0.000	0.000	0	1	0.529	0.011
NGC 4957	13:02:48	+27:50:14	-5	14.27	0	2	6921	57	2.361	0.017	0	1	0.305	0.008	0	2	0.417	0.017
NGC 4971	13:04:31	+28:48:45	-5	15.26	0	1	6307	51	2.264	0.024	0	0	0.000	0.000	0	1	0.294	0.011
NGC 5004	13:08:39	+29:54:07	-2	14.30	0	1	6960	55	2.385	0.027	0	0	0.000	0.000	0	1	0.497	0.011
CGCG 160-159	13:09:44	+27:35:35	-5	15.00	0	1	6136	50	2.374	0.022	0	0	0.000	0.000	0	1	0.295	0.011
HG50																		
NGC 5813	14:58:42	+01:54:00	-5	12.09	5	2	1954	17	2.372	0.009	5	1	0.305	0.008	2	1	0.920	0.005
NGC 5831	15:01:36	+01:25:00	-5	13.05	0	2	1683	13	2.260	0.021	0	1	0.293	0.011	1	1	0.790	0.010
NGC 5839	15:02:54	+01:50:00	-2	13.90	0	1	1211	24	2.140	0.027	0	0	0.000	0.000	1	0	0.660	0.009
NGC 5838	15:02:54	+02:18:00	-3	12.14	0	1	1359	10	2.453	0.040	0	1	0.000	0.000	1	0	0.970	0.009
NGC 5845	15:03:28	+01:49:36	-5	13.51	1	3	1450	19	2.394	0.013	1	1	0.297	0.011	2	1	0.746	0.005
NGC 5846	15:03:56	+01:47:48	-5	11.76	1	4	1723	30	2.416	0.012	1	1	0.325	0.002	1	1	1.018	0.010
NGC 5865	15:07:18	+00:39:00	-2	13.50	0	1	2110	16	2.394	0.054	0	0	0.000	0.000	1	0	0.740	0.005
A2199																		
NGC 6146	16:23:30	+41:01:00	-5	13.54	0	1	8738	71	2.446	0.025	0	1	0.293	0.008	0	1	0.590	0.011
NGC 6158	16:25:58	+39:29:35	-5	14.73	0	2	8980	71	2.282	0.020	0	2	0.277	0.002	0	2	0.343	0.011
NGC 6160	16:26:00	+41:02:00	-5	13.94	0	1	9408	77	2.380	0.028	0	1	0.299	0.009	0	1	0.370	0.011
PGC 058213	16:26:13	+39:40:40	-5	16.63	0	1	9398	76	2.182	0.027	0	1	0.000	0.000	0	1	0.132	0.011

Table 7—Continued

Name	α	δ	T	m_B	N_s^o	N_s^l	cz_{hel}	$\epsilon_{cz_{hel}}$	$\log \sigma$	$\epsilon_{\log \sigma}$	N_M^o	N_M^l	M_{g2}	$\epsilon_{M_{g2}}$	N_d^o	N_d^l	$\log d_n$	$\epsilon_{\log d_n}$
(1)	(2)	(3)	(4)	(5)	(6)	(7)	(8)	(9)	(10)	(11)	(12)	(13)	(14)	(15)	(16)	(17)	(18)	(19)
1626+3937	16:26:25	+39:37:57	-2	17.00	0	1	9147	74	2.334	0.026	0	1	0.000	0.000	0	1	0.058	0.011
NGC 6166C	16:26:40	+39:40:50	-5	15.45	0	1	8806	72	2.246	0.019	0	1	0.288	0.001	0	2	0.144	0.005
MCG +07-34-049	16:26:41	+39:42:53	-3	16.44	0	1	9407	75	2.350	0.025	0	0	0.000	0.000	0	1	0.110	0.011
MCG +07-34-055	16:26:53	+39:38:34	-5	16.23	0	2	8497	69	2.380	0.011	0	1	0.271	0.007	0	3	0.153	0.005
MCG +07-34-065	16:27:01	+39:35:36	-2	16.25	0	1	10162	81	2.060	0.037	0	2	0.000	0.000	0	1	-0.090	0.011
MCG +07-34-070	16:27:03	+39:38:11	-5	16.82	0	2	8259	68	2.186	0.015	0	1	0.275	0.002	0	3	-0.002	0.015
MCG +07-34-074	16:27:07	+39:43:28	-5	17.16	0	2	9215	74	2.290	0.016	0	1	0.302	0.001	0	3	0.070	0.005
PGC 058301	16:27:15	+39:49:01	-5	16.43	0	2	9400	78	2.283	0.022	0	2	0.302	0.002	0	2	0.100	0.011
NGC 6173	16:28:06	+40:55:00	-5	13.19	0	1	8800	72	2.427	0.023	0	1	0.336	0.012	0	1	0.550	0.011
Pegasus																		
NGC 7612	23:17:12	+08:18:09	-2	14.30	0	1	3228	25	2.299	0.052	0	1	0.000	0.000	1	0	0.630	0.008
NGC 7619	23:17:42	+07:55:57	-5	12.78	1	2	3775	28	2.525	0.012	1	2	0.337	0.004	0	1	0.830	0.011
NGC 7623	23:17:58	+08:07:20	-2	14.17	1	0	3628	46	2.324	0.039	1	0	0.282	0.011	1	0	0.610	0.009
NGC 7626	23:18:10	+07:56:36	-5	12.90	2	2	3409	19	2.417	0.011	2	2	0.329	0.008	1	1	0.823	0.017
A2634																		
CGCG 476-085	23:35:48	+26:36:35	-5	14.86	0	2	9348	74	2.412	0.019	0	1	0.276	0.010	0	2	0.186	0.011
2335+2645	23:35:48	+26:45:30	-5	17.01	0	2	9552	76	2.256	0.017	0	1	0.285	0.001	0	3	0.033	0.008
CGCG 476-086	23:35:52	+26:52:53	-5	14.82	0	1	9332	75	2.314	0.021	0	1	0.265	0.010	0	2	0.217	0.011
CGCG 476-087	23:35:56	+26:42:30	-2	15.20	0	1	10873	70	2.302	0.020	0	1	0.316	0.011	0	1	0.228	0.011
CGCG 476-090	23:35:59	+26:42:07	-5	15.20	0	1	9538	76	2.361	0.013	0	1	0.326	0.001	0	3	0.255	0.015
CGCG 476-092	23:36:04	+26:42:09	-2	17.14	0	1	8556	69	2.351	0.019	0	1	0.314	0.008	0	2	0.158	0.011
2336+2645	23:36:06	+26:45:10	-2	16.94	0	2	8491	68	2.311	0.016	0	1	0.302	0.002	0	3	0.157	0.008
IC 5342	23:36:08	+26:44:03	-5	16.76	0	2	9293	75	2.360	0.013	0	1	0.300	0.012	0	3	0.246	0.008
2336+2650a	23:36:12	+26:50:30	-2	16.67	0	2	9554	76	2.245	0.019	0	1	0.279	0.010	0	2	0.040	0.011
2336+2650b	23:36:19	+26:50:46	-2	16.80	0	2	8990	71	2.247	0.022	0	1	0.263	0.009	0	2	0.020	0.011
2336+2646	23:36:23	+26:46:08	-2	16.84	0	1	9643	77	2.143	0.035	0	1	0.258	0.012	0	2	-0.003	0.011
2336+2653	23:36:26	+26:53:06	-2	17.28	0	2	9217	74	2.241	0.019	0	1	0.285	0.008	0	2	0.103	0.011
A194																		
IC 1696	01:22:19	-01:52:37	-5	14.62	0	2	5827	48	2.233	0.018	0	2	0.300	0.003	1	2	0.366	0.012
0122-0127	01:22:50	-01:27:17	-5	16.58	0	1	5242	42	1.898	0.036	0	1	0.000	0.000	1	0	0.030	0.011
CGCG 385-123	01:22:59	-01:45:44	-2	15.36	0	2	5785	45	2.152	0.016	0	1	0.254	0.010	1	3	0.362	0.005
CGCG 385-126	01:23:11	-01:43:01	-2	15.41	0	3	5237	42	2.194	0.013	0	1	0.259	0.011	1	3	0.354	0.005
NGC 0541	01:23:11	-01:38:22	-3	14.00	4	5	5404	18	2.329	0.009	4	2	0.330	0.008	3	3	0.538	0.005
PGC 005306	01:23:15	-01:45:06	-2	16.70	0	2	5178	42	1.896	0.036	0	1	0.000	0.000	1	1	-0.052	0.015
NGC 0543	01:23:16	-01:33:09	-2	15.51	0	3	5318	43	2.373	0.012	0	1	0.315	0.009	2	3	0.365	0.005
0123-0131	01:23:19	-01:31:34	-5	16.72	0	2	6300	51	1.995	0.018	0	1	0.206	0.012	3	3	0.077	0.005
NGC 0548	01:23:29	-01:29:06	-3	14.62	0	2	5419	45	2.182	0.015	0	2	0.254	0.008	1	3	0.226	0.005
0123-0150	01:23:58	-01:50:02	-2	16.82	0	1	5509	45	1.929	0.038	0	1	0.000	0.000	2	0	-0.070	0.015
CGCG 385-144	01:24:43	-01:31:51	-2	15.27	0	2	4804	39	2.217	0.015	0	1	0.270	0.012	1	3	0.334	0.006
NGC 0560	01:24:54	-02:10:00	-3	14.41	1	1	5456	31	2.344	0.018	0	1	0.283	0.010	0	1	0.533	0.011
CGCG 385-146	01:25:02	-01:21:49	-2	15.10	0	1	4489	36	2.073	0.033	0	1	0.233	0.011	0	1	0.333	0.011
NGC 0564	01:25:12	-02:08:00	-5	14.02	0	2	5836	45	2.383	0.016	0	2	0.303	0.009	0	2	0.541	0.012
CGCG 385-151	01:25:28	-00:59:50	-2	15.60	0	1	5712	45	1.958	0.032	0	1	0.201	0.011	0	1	0.153	0.011
Fornax																		
ESO 357G022	03:20:47	-37:23:12	-2	9.93	3	2	1739	21	2.341	0.014	3	0	0.252	0.004	1	1	1.330	0.015
NGC 1336	03:24:35	-35:53:18	-2	13.80	2	0	1447	30	1.911	0.028	2	0	0.185	0.011	1	0	0.420	0.008
ESO 418G004	03:26:06	-32:27:30	-5	12.63	1	2	1331	47	2.202	0.017	1	2	0.301	0.002	2	2	0.775	0.005
ESO 418G005	03:26:17	-31:14:24	-5	11.51	1	1	1205	25	2.212	0.020	1	1	0.259	0.002	0	1	1.030	0.011
ESO 358G012	03:28:38	-35:01:24	-2	12.91	1	1	1723	49	2.156	0.024	1	1	0.270	0.011	0	1	0.780	0.011

Table 7—Continued

Name	α	δ	T	m_B	N_s^o	N_s^l	$c_{z_{hel}}$	$\epsilon_{c_{z_{hel}}}$	$\log \sigma$	$\epsilon_{\log \sigma}$	N_M^o	N_M^l	M $_{g2}$	$\epsilon_{M_{g2}}$	N_d^o	N_d^l	$\log d_n$	$\epsilon_{\log d_n}$
(1)	(2)	(3)	(4)	(5)	(6)	(7)	(8)	(9)	(10)	(11)	(12)	(13)	(14)	(15)	(16)	(17)	(18)	(19)
ESO 418G010	03:31:52	-31:21:36	-2	13.13	1	0	1258	52	2.057	0.023	1	0	0.267	0.010	1	0	0.760	0.005
ESO 358G021	03:33:03	-35:20:13	-5	14.27	1	0	1383	17	1.772	0.037	1	0	0.184	0.011	1	0	0.410	0.005
ESO 358G023	03:33:21	-35:23:30	-2	12.56	1	1	1320	32	2.228	0.022	1	1	0.296	0.011	1	1	0.847	0.007
ESO 358G025	03:33:34	-32:37:48	-2	14.10	1	0	1437	19	1.739	0.041	1	0	0.113	0.011	2	0	0.410	0.005
IC 1963	03:33:34	-34:36:44	-5	13.16	2	0	1640	19	1.930	0.029	2	0	0.220	0.008	1	0	0.650	0.008
ESO 358G027	03:34:08	-35:36:18	-5	12.33	2	1	1347	15	2.060	0.019	2	1	0.254	0.007	1	2	0.833	0.008
ESO 358G028	03:34:32	-35:08:24	-2	11.36	0	1	1844	14	2.356	0.036	0	2	0.000	0.000	1	0	1.130	0.008
ESO 358G038	03:35:17	-35:54:30	-2	12.65	1	1	948	38	2.119	0.025	1	1	0.236	0.002	1	1	0.813	0.013
ESO 358G045	03:36:34	-35:36:42	-5	11.11	1	2	1425	39	2.520	0.014	1	2	0.335	0.002	2	2	1.164	0.006
ESO 358G046	03:36:57	-35:45:18	-5	11.46	1	1	1916	26	2.389	0.020	1	1	0.315	0.005	2	1	1.160	0.005
ESO 301G023	03:38:51	-37:40:18	-5	14.30	1	1	1574	23	2.087	0.019	1	0	0.227	0.010	1	1	0.593	0.013
ESO 358G052	03:40:25	-35:33:06	-2	12.20	1	1	1410	15	2.209	0.021	1	1	0.249	0.011	2	1	0.857	0.005
ESO 358G059	03:43:10	-36:07:42	-5	14.10	2	0	1043	21	1.659	0.050	2	1	0.152	0.008	1	1	0.403	0.005
Eridanus																		
ESO 480G028	03:01:58	-26:15:42	-5	11.84	1	1	1680	24	2.217	0.025	1	0	0.305	0.011	1	0	0.950	0.006
ESO 547G030	03:16:58	-19:16:54	-2	12.87	5	0	1579	26	2.037	0.015	5	0	0.289	0.011	1	0	0.530	0.005
ESO 548G003	03:20:53	-21:33:12	-2	13.70	1	0	1611	2	1.750	0.041	1	0	0.202	0.011	2	0	0.430	0.005
ESO 548G018	03:24:04	-21:30:36	-2	11.46	0	2	1550	12	2.514	0.016	0	0	0.000	0.000	2	0	1.077	0.005
ESO 548G019	03:24:15	-21:31:48	-3	14.46	1	0	1204	61	1.741	0.043	1	0	0.179	0.011	1	1	0.360	0.020
ESO 548G041	03:31:39	-20:26:54	-2	14.00	1	0	1176	30	1.960	0.037	1	0	0.223	0.011	2	0	0.460	0.006
ESO 482G019	03:36:19	-23:11:24	-5	11.44	1	3	1725	33	2.404	0.011	1	2	0.320	0.002	3	1	1.071	0.005
ESO 482G026	03:37:11	-22:53:06	-2	13.40	1	0	1495	23	1.918	0.034	1	0	0.209	0.011	1	0	0.620	0.005
ESO 548G067	03:37:57	-18:44:30	-3	11.06	1	2	1814	30	2.445	0.011	1	1	0.329	0.003	3	1	1.062	0.005
ESO 548G068	03:38:04	-19:05:30	-2	14.20	2	0	1693	18	2.018	0.025	2	0	0.196	0.011	1	0	0.380	0.007
ESO 549G001	03:40:38	-22:16:06	-5	12.57	3	2	1437	16	2.175	0.010	3	2	0.259	0.007	2	2	0.765	0.005
ESO 549G009	03:42:39	-22:04:42	-5	12.84	1	2	1673	22	2.164	0.013	1	2	0.277	0.003	1	2	0.715	0.005
Doradus																		
ESO 201G020	04:06:56	-48:01:42	-2	11.96	0	1	1174	24	2.196	0.030	0	1	0.260	0.010	0	1	0.943	0.011
ESO 250G007	04:07:28	-45:38:54	-5	12.44	3	0	1492	32	2.018	0.021	3	0	0.197	0.016	0	1	0.910	0.011
ESO 157G016	04:14:39	-55:42:54	-3	11.13	0	2	1238	24	2.309	0.022	0	2	0.307	0.011	2	2	1.132	0.007
ESO 157G022	04:20:59	-57:05:24	-2	11.56	0	1	1050	23	2.334	0.032	0	1	0.287	0.011	1	1	1.058	0.005
A3381																		
0604-3348	06:04:58	-33:48:29	-3	14.73	1	1	11488	22	2.346	0.023	1	1	0.303	0.011	0	1	0.293	0.011
0607-3335	06:07:60	-33:35:09	-2	15.00	0	1	11306	35	2.340	0.028	0	1	0.309	0.011	0	1	0.098	0.011
MCG -06-14-005	06:08:05	-33:34:53	-2	15.50	0	1	11557	43	2.334	0.029	0	1	0.322	0.010	1	1	0.178	0.005
0608-3328	06:08:21	-33:28:08	-5	15.00	0	1	11463	30	2.337	0.026	0	1	0.269	0.010	0	1	0.158	0.011
PGC 018554	06:08:49	-33:30:55	-2	15.00	0	1	11487	28	2.136	0.025	0	1	0.187	0.015	0	1	-0.042	0.030
0609-3343	06:09:06	-33:43:29	-2	15.79	1	1	11680	25	2.331	0.019	1	1	0.262	0.011	0	1	0.261	0.029
Hydra																		
ESO 436G027	10:26:36	-31:21:12	-2	12.99	1	0	4231	26	2.382	0.022	1	0	0.255	0.008	1	0	0.730	0.005
ESO 501G003	10:29:27	-26:18:30	-3	14.03	2	1	4172	15	2.353	0.013	2	1	0.287	0.002	3	1	0.486	0.008
ESO 501G013	10:31:09	-26:38:24	-2	14.20	1	1	3589	42	2.354	0.020	1	1	0.296	0.010	1	1	0.534	0.014
PGC 031288	10:32:15	-28:18:33	-2	15.36	1	0	3522	37	2.230	0.020	1	0	0.285	0.011	1	1	0.331	0.005
ESO 436G044	10:32:27	-28:14:24	-2	14.16	0	1	3221	26	2.232	0.026	0	1	0.258	0.009	1	1	0.561	0.005
ESO 436G045	10:32:30	-28:15:30	-5	15.35	0	1	3402	28	2.298	0.031	0	1	0.268	0.010	1	1	0.344	0.005
ESO 501G025	10:33:04	-26:23:54	-2	14.41	1	0	3821	13	2.125	0.019	1	0	0.269	0.009	1	0	0.330	0.005
PGC 031407	10:33:43	-27:14:58	-5	15.08	0	2	2286	19	2.033	0.019	0	1	0.240	0.010	1	3	0.208	0.010
ESO 501G030	10:33:51	-26:54:12	-5	14.14	1	3	3975	18	2.375	0.012	1	1	0.325	0.011	2	4	0.589	0.011
PGC 031422	10:33:52	-27:25:44	-2	15.59	0	1	4196	34	1.945	0.032	0	1	0.000	0.000	1	1	0.012	0.018

Table 7—Continued

Name	α	δ	T	m_B	N_s^o	N_s^l	cz_{hel}	$\epsilon_{cz_{hel}}$	$\log \sigma$	$\epsilon_{\log \sigma}$	N_M^o	N_M^l	Mg2	ϵ_{Mg2}	N_d^o	N_d^l	$\log d_n$	$\epsilon_{\log d_n}$	
(1)	(1950)	(1950)	(4)	mag	(6)	(7)	kms ⁻¹	kms ⁻¹	(10)	(11)	(12)	(13)	(14)	(15)	(16)	(17)	(18)	(19)	
1033-2654	10:33:59	-26:54:25	-2	16.53	0	1	3687	30	1.888	0.038	0	0	0.000	0.000	1	1	-0.083	0.015	
PGC 031432	10:33:58	-27:27:42	-2	15.49	0	1	3551	29	1.935	0.045	0	1	0.000	0.000	1	1	0.023	0.007	
ESO 501G034	10:34:01	-27:10:42	-2	13.55	1	1	3555	59	2.293	0.011	1	2	0.305	0.002	5	4	0.597	0.007	
PGC 031441	10:34:02	-27:05:41	-2	15.19	2	1	3026	24	2.102	0.013	2	1	0.249	0.011	1	3	0.244	0.008	
ESO 501G035	10:34:03	-26:44:24	-2	14.21	1	0	4202	44	2.146	0.071	1	0	0.250	0.011	1	0	0.430	0.005	
PGC 031444	10:34:04	-27:19:20	-3	15.46	0	1	2816	23	1.987	0.034	0	2	0.000	0.000	1	1	0.093	0.007	
PGC 031447	10:34:06	-27:03:33	-2	14.93	2	1	3368	35	2.277	0.014	2	1	0.279	0.006	1	3	0.414	0.005	
PGC 031450	10:34:08	-27:13:28	-2	15.00	0	2	4776	39	2.048	0.025	0	2	0.000	0.000	3	2	0.121	0.005	
ESO 437G009	10:34:14	-27:57:24	-3	14.74	1	0	3654	48	2.088	0.046	1	0	0.254	0.011	2	1	0.424	0.030	
ESO 501G036	10:34:15	-27:15:30	-5	12.24	1	1	4082	24	2.443	0.008	1	2	0.332	0.005	2	2	0.754	0.005	
PGC 031476	10:34:20	-27:18:04	-5	14.97	0	2	4739	38	2.085	0.018	0	1	0.283	0.012	1	3	0.292	0.005	
PGC 031483	10:34:24	-27:12:35	-5	15.13	0	1	2703	22	2.332	0.018	0	1	0.000	0.000	2	2	0.362	0.005	
D195	10:34:28	-27:07:44	-5	16.03	1	1	4475	18	1.999	0.021	1	0	0.248	0.011	1	1	-0.031	0.015	
ESO 437G011	10:34:29	-27:39:37	-2	14.22	0	1	4938	40	2.275	0.025	0	1	0.285	0.008	1	1	0.508	0.005	
ESO 437G013	10:34:33	-27:39:28	-2	14.58	0	1	3499	28	2.220	0.023	0	1	0.249	0.011	1	1	0.484	0.006	
D135	10:34:48	-27:23:52	-5	15.60	0	2	4115	33	2.068	0.025	0	2	0.000	0.000	1	2	0.204	0.005	
ESO 501G047	10:34:56	-27:12:31	-2	14.18	0	2	4820	39	2.104	0.018	0	1	0.287	0.012	0	2	0.360	0.008	
ESO 501G048	10:34:58	-26:55:54	-2	14.12	0	1	3840	31	2.250	0.017	0	1	0.249	0.011	0	2	0.530	0.008	
ESO 501G049	10:34:59	-27:17:57	-2	15.05	0	1	4014	33	2.050	0.020	0	1	0.237	0.011	2	2	0.214	0.005	
PGC 031577	10:35:19	-26:47:51	-2	15.46	1	1	4381	24	1.919	0.021	1	1	0.212	0.011	1	1	0.248	0.008	
ESO 501G056	10:35:23	-26:22:12	-2	14.05	1	0	3580	62	2.349	0.022	1	0	0.258	0.011	1	0	0.590	0.005	
ESO 501G058	10:35:26	-26:49:18	-2	13.01	0	2	2940	24	2.314	0.021	0	1	0.318	0.010	1	1	0.714	0.014	
D119	10:35:40	-27:11:27	-2	15.87	0	2	5247	42	2.036	0.023	0	2	0.000	0.000	1	2	0.176	0.005	
ESO 437G021	10:35:50	-28:31:24	-2	14.26	2	1	3903	23	2.249	0.013	2	1	0.287	0.003	1	1	0.504	0.005	
NGC 3335	10:37:11	-23:39:42	-2	14.02	1	0	3862	66	2.106	0.042	1	0	0.291	0.008	1	0	0.510	0.008	
PGC 031765	10:38:03	-27:37:12	-2	14.26	1	0	4515	12	1.856	0.046	1	0	0.114	0.011	0	1	0.253	0.011	
(RMH82) 64	10:38:11	-27:36:00	-2	14.62	1	0	3964	28	1.988	0.036	1	0	0.183	0.011	0	1	0.203	0.011	
ESO 437G038	10:38:29	-27:42:10	-2	14.47	1	0	4477	33	2.295	0.018	1	0	0.236	0.010	1	1	0.441	0.005	
ESO 437G045	10:39:38	-28:30:54	-2	14.26	3	1	3718	22	2.185	0.017	3	1	0.275	0.002	1	1	0.434	0.005	
AS639																			
ESO 264G023	10:36:59	-46:14:40	-2	14.46	0	1	5658	46	2.337	0.028	0	1	0.292	0.009	0	1	0.453	0.011	
1037-4555	10:37:49	-45:55:46	-5	14.71	0	1	6627	54	2.287	0.031	0	1	0.263	0.010	1	1	0.513	0.011	
1037-4553	10:37:52	-45:53:26	-2	—	0	1	5647	44	2.133	0.023	0	1	0.244	0.015	0	1	0.388	0.013	
1037-4607	10:37:52	-46:07:24	-5	16.14	0	1	5854	47	2.100	0.031	0	1	0.207	0.010	2	1	0.244	0.005	
1038-4604	10:38:02	-46:04:54	-2	—	0	1	6140	49	2.470	0.021	0	1	0.315	0.011	2	1	0.541	0.021	
ESO 264G031	10:38:23	-45:55:46	-3	13.35	0	2	6694	55	2.396	0.019	0	2	0.288	0.005	1	2	0.573	0.018	
Cen45																			
ESO 322G056	12:39:33	-40:22:06	-2	14.41	0	1	4580	37	2.246	0.031	0	1	0.268	0.010	0	1	0.530	0.011	
ESO 322G075	12:43:41	-40:28:48	-2	14.11	0	1	4738	37	2.181	0.017	0	1	0.263	0.012	0	1	0.610	0.008	
ESO 322G099	12:46:40	-41:13:02	-2	14.74	0	2	4277	35	2.078	0.022	0	1	0.000	0.000	0	2	0.489	0.008	
ESO 322G100	12:46:41	-41:11:27	-2	14.62	0	2	4831	39	2.032	0.024	0	1	0.000	0.000	0	2	0.389	0.008	
ESO 323G003	12:47:18	-41:06:36	-2	12.74	0	1	4624	22	2.420	0.015	0	1	0.333	0.005	0	2	0.805	0.005	
ESO 323G008	12:47:48	-41:11:57	-2	14.83	0	2	5312	43	2.128	0.023	0	2	0.000	0.000	0	2	0.459	0.008	
ESO 323G023	12:49:40	-40:26:12	-2	14.45	0	1	4430	34	2.184	0.021	0	1	0.293	0.010	0	1	0.500	0.008	
ESO 323G034	12:50:39	-40:56:00	-5	13.28	0	1	4330	34	2.397	0.022	0	1	0.297	0.011	0	1	0.800	0.011	
Cen30																			
ESO 322G014	12:24:57	-39:03:42	-5	12.25	0	1	2924	24	2.301	0.018	0	1	0.000	0.000	0	1	0.895	0.005	
ESO 322G038	12:35:35	-41:13:36	-2	13.94	0	1	3165	26	2.323	0.016	0	1	0.311	0.008	0	1	0.640	0.008	
ESO 322G051	12:38:10	-41:19:54	-2	14.22	1	1	3239	24	2.282	0.017	1	1	0.329	0.011	1	1	0.625	0.009	

Table 7—Continued

Name	α	δ	T	m_B	N_s^o	N_s^l	cz_{hel}	$\epsilon_{cz_{hel}}$	$\log \sigma$	$\epsilon_{\log \sigma}$	N_M^o	N_M^l	M _{g2}	ϵ_{Mg2}	N_d^o	N_d^l	$\log d_n$	$\epsilon_{\log d_n}$
(1)	(2)	(3)	(4)	(5)	(6)	(7)	(8)	(9)	(10)	(11)	(12)	(13)	(14)	(15)	(16)	(17)	(18)	(19)
ESO 322G060	12:40:47	-41:05:18	-2	13.68	1	1	2718	79	2.243	0.018	1	1	0.286	0.011	1	1	0.770	0.012
ESO 322G066	12:41:25	-41:28:36	-5	13.08	0	1	2652	22	2.287	0.019	0	1	0.281	0.010	0	1	0.830	0.008
NGC 4661	12:42:19	-40:44:24	-5	14.74	0	1	2566	22	2.176	0.024	0	1	0.268	0.012	0	1	0.373	0.011
ESO 322G081	12:44:36	-40:57:54	-2	14.10	0	2	2993	24	2.388	0.015	0	1	0.279	0.009	0	2	0.688	0.005
ESO 322G089	12:45:37	-40:51:03	-5	15.42	0	2	3685	29	2.150	0.021	0	0	0.000	0.000	0	2	0.368	0.008
PGC 043269	12:45:45	-41:02:03	-5	16.62	0	1	3001	25	1.945	0.035	0	1	0.000	0.000	0	1	0.080	0.011
NGC 4696	12:46:04	-41:02:18	-2	11.47	0	2	3008	25	2.418	0.014	0	1	0.283	0.002	0	2	0.914	0.005
PGC 043340	12:46:33	-41:03:48	-5	16.17	0	1	3134	25	1.930	0.034	0	1	0.000	0.000	0	1	0.105	0.011
PGC 043402	12:47:06	-40:57:16	-5	16.18	1	2	2192	15	2.109	0.017	2	1	0.268	0.005	0	2	0.373	0.008
ESO 323G001	12:47:08	-41:00:30	-2	14.26	0	2	3862	30	2.348	0.014	0	1	0.315	0.008	0	2	0.636	0.005
PGC 043433	12:47:25	-40:56:57	-5	15.72	1	2	2999	60	2.076	0.020	1	1	0.283	0.011	0	2	0.331	0.008
PGC 043434	12:47:26	-41:01:38	-5	16.00	0	1	4172	33	1.859	0.037	0	0	0.000	0.000	0	1	-0.017	0.011
ESO 323G009	12:47:57	-41:09:31	-2	14.96	0	2	2385	20	2.106	0.024	0	1	0.000	0.000	0	2	0.436	0.008
ESO 323G015	12:48:59	-38:33:30	-2	14.16	0	1	3140	26	2.172	0.021	0	1	0.241	0.009	0	1	0.460	0.008
ESO 323G016	12:49:00	-40:51:36	-3	13.75	0	1	3344	19	2.208	0.019	0	1	0.270	0.011	1	1	0.663	0.005
ESO 323G017	12:49:14	-40:52:30	-2	14.16	8	0	2106	16	2.307	0.008	8	0	0.299	0.006	1	0	0.600	0.008
ESO 323G021	12:49:29	-41:07:06	-2	14.26	0	1	3014	25	2.098	0.022	0	1	0.258	0.010	0	1	0.590	0.008
ESO 323G036	12:51:07	-39:26:36	-5	12.88	0	1	2976	24	2.330	0.017	0	1	0.289	0.005	0	1	0.850	0.008
AS714																		
ESO 507G014	12:45:40	-26:11:30	-2	13.92	1	0	3294	67	2.164	0.037	1	0	0.266	0.011	1	0	0.610	0.005
ESO 507G019	12:47:22	-25:38:54	-2	13.72	1	0	3264	56	2.250	0.021	1	0	0.314	0.010	1	0	0.610	0.006
ESO 507G021	12:47:48	-26:34:12	-2	13.51	1	0	3185	28	2.309	0.027	1	0	0.326	0.010	1	0	0.640	0.005
ESO 507G025	12:48:51	-26:10:48	-2	12.73	0	1	3239	26	2.404	0.015	0	1	0.298	0.004	0	1	0.840	0.008
ESO 507G027	12:48:57	-25:50:42	-2	13.77	1	0	3199	24	2.285	0.028	1	0	0.277	0.009	1	0	0.640	0.008
ESO 507G032	12:49:34	-26:01:54	-2	13.81	1	0	3465	20	2.343	0.029	1	0	0.273	0.009	1	0	0.630	0.008
ESO 507G055	12:54:55	-27:01:18	-2	13.65	0	1	3320	27	2.202	0.019	0	1	0.282	0.009	1	1	0.605	0.005
Klemola27																		
MCG -05-32-74	13:42:31	-29:46:04	-2	14.39	4	0	4403	11	2.259	0.016	4	0	0.283	0.006	1	1	0.378	0.008
ESO 445G028	13:44:27	-29:33:36	-5	14.30	2	1	4514	41	2.389	0.013	2	1	0.298	0.006	1	1	0.534	0.005
ESO 445G040	13:45:48	-30:33:48	-2	14.45	1	1	5080	77	2.122	0.016	1	1	0.257	0.002	1	1	0.364	0.005
ESO 445G046	13:46:14	-30:02:54	-3	12.22	5	3	4551	22	2.470	0.007	5	2	0.321	0.004	2	2	0.715	0.021
(WFC91) 074	13:47:54	-29:45:04	-2	14.77	0	1	4301	34	2.339	0.025	0	1	0.299	0.008	1	1	0.420	0.011
(WFC91) 079	13:48:19	-30:15:48	-5	15.89	1	0	4753	10	2.002	0.035	1	0	0.192	0.007	1	0	0.070	0.005
ESO 445G059	13:48:47	-30:14:31	-2	13.65	1	1	4535	19	2.302	0.016	1	1	0.295	0.006	1	1	0.511	0.005
ESO 445G062	13:49:16	-30:12:18	-2	15.43	1	0	4705	20	1.972	0.031	1	0	0.215	0.011	1	1	0.154	0.005
ESO 445G065	13:49:54	-29:40:59	-2	14.11	1	0	4774	11	2.238	0.022	1	0	0.272	0.010	1	0	0.530	0.008
ESO 445G078	13:53:07	-30:05:48	-2	13.35	0	1	4975	40	2.329	0.018	0	1	0.251	0.002	0	1	0.695	0.005
AS753																		
ESO 384G013	13:52:47	-33:28:54	-2	14.23	1	1	3768	37	1.969	0.026	1	1	0.194	0.008	0	1	0.450	0.011
ESO 384G019	13:54:44	-33:58:30	-2	12.92	1	1	4267	15	2.183	0.018	1	1	0.267	0.007	2	1	0.580	0.005
(WFC91) 010	13:55:45	-33:13:32	-2	15.29	0	1	3986	31	2.118	0.031	0	1	0.226	0.010	1	1	0.358	0.005
(WFC91) 012	13:55:56	-33:14:52	-2	14.84	0	1	4166	33	2.222	0.036	0	1	0.282	0.012	1	1	0.398	0.005
(WFC91) 017	13:56:55	-34:04:31	-5	15.17	1	1	4189	35	2.005	0.023	1	1	0.212	0.011	0	1	0.283	0.011
ESO 384G026	13:57:19	-33:47:42	-2	14.49	1	0	4426	30	2.306	0.019	1	0	0.307	0.012	1	0	0.540	0.006
(WFC91) 037	13:59:14	-33:32:59	-2	14.93	0	1	3883	31	2.240	0.027	0	1	0.298	0.009	2	1	0.401	0.005
(WFC91) 045	13:59:47	-34:43:20	-2	15.83	1	0	4100	21	1.875	0.036	1	0	0.176	0.011	0	1	0.043	0.011
(WFC91) 047	13:59:57	-34:00:56	-2	15.05	0	1	4190	33	2.087	0.034	0	1	0.249	0.011	0	1	0.363	0.011
(WFC91) 049	14:00:10	-33:47:30	-2	14.57	0	1	5214	41	2.409	0.025	0	1	0.302	0.008	0	1	0.493	0.011
(WFC91) 051	14:00:11	-33:51:30	-5	14.67	0	1	3978	31	2.191	0.031	0	1	0.247	0.010	0	1	0.333	0.011

Table 7—Continued

Name	α (1950)	δ (1950)	T	m_B mag	N_s^o	N_s^l	$c_{z_{hel}}$ kms $^{-1}$	$\epsilon_{c_{z_{hel}}}$ kms $^{-1}$	$\log \sigma$	$\epsilon_{\log \sigma}$	N_M^o	N_M^l	M_{G2}	$\epsilon_{M_{G2}}$	N_d^o	N_d^l	$\log d_n$	$\epsilon_{\log d_n}$	
(1)	(2)	(3)	(4)	(5)	(6)	(7)	(8)	(9)	(10)	(11)	(12)	(13)	(14)	(15)	(16)	(17)	(18)	(19)	
ESO 384G039	14:00:42	-33:44:18	-2	12.03	6	3	4150	28	2.540	0.007	6	2	0.336	0.004	2	2	0.887	0.005	
(WFC91) 065	14:00:43	-33:56:35	-2	16.01	1	0	4505	18	1.958	0.030	1	0	0.261	0.011	2	0	0.060	0.005	
MCG -06-31-020	14:01:36	-33:43:17	-2	14.01	0	1	3855	30	2.280	0.033	0	1	0.301	0.011	2	1	0.515	0.007	
ESO 384G049	14:03:10	-33:41:05	-2	14.16	0	2	4441	35	2.283	0.020	0	2	0.289	0.005	1	2	0.508	0.005	
(WFC91) 083	14:03:10	-32:57:58	-2	15.30	2	0	4111	23	2.009	0.026	2	0	0.247	0.002	1	0	0.290	0.008	
(WFC91) 095	14:03:52	-34:15:13	-5	14.90	0	1	4701	37	2.131	0.028	0	1	0.259	0.009	0	1	0.343	0.011	
(WFC91) 103	14:04:57	-34:03:56	-2	15.73	1	0	4439	17	1.994	0.031	1	0	0.184	0.011	1	0	0.160	0.008	
PavoII																			
NGC 6545	18:07:26	-63:47:18	-5	14.19	1	0	4282	32	2.193	0.022	1	0	0.254	0.010	1	0	0.505	0.005	
NGC 6614	18:20:22	-63:16:30	-3	13.80	2	0	4351	48	2.390	0.019	2	0	0.312	0.012	1	0	0.610	0.005	
IC 4727	18:33:15	-62:44:36	-3	14.06	1	0	4499	44	2.312	0.024	1	0	0.307	0.011	1	0	0.560	0.006	
IC 4731	18:34:00	-62:59:12	-2	12.84	2	0	4519	21	2.293	0.021	2	0	0.288	0.011	1	0	0.700	0.008	
IC 4742	18:37:05	-63:54:36	-5	13.09	0	1	4435	38	2.343	0.016	0	1	0.000	0.000	0	1	0.600	0.008	
PGC 062384	18:41:40	-63:22:42	-2	14.00	1	2	3636	40	2.074	0.019	1	0	0.265	0.009	0	1	0.246	0.008	
ESO 104G002	18:42:09	-63:24:53	-2	15.03	1	2	4184	22	2.088	0.021	1	0	0.273	0.008	0	2	0.237	0.008	
ESO 104G007	18:42:34	-63:24:54	-5	13.79	0	1	4034	30	2.353	0.015	0	1	0.000	0.000	0	2	0.592	0.008	
IC 4765	18:42:34	-63:23:12	-3	12.33	0	2	4498	35	2.483	0.012	0	1	0.332	0.011	0	3	0.661	0.007	
IC 4784	18:48:05	-63:19:18	-3	13.73	0	1	4884	39	2.429	0.016	0	0	0.000	0.000	0	1	0.550	0.008	
IC 4801	18:54:48	-64:44:36	-2	13.62	1	0	4447	12	2.275	0.028	1	0	0.298	0.012	1	0	0.630	0.008	
NGC 6733	19:01:35	-62:16:24	-3	13.41	0	1	4881	39	2.401	0.015	0	1	0.000	0.000	0	1	0.590	0.008	
Klemola44																			
2344-2831	23:44:02	-28:31:51	-5	16.86	0	1	8005	65	1.994	0.035	0	0	0.000	0.000	0	1	-0.027	0.011	
PGC 072393	23:44:36	-28:12:28	-2	16.14	2	1	8796	35	2.039	0.024	2	0	0.289	0.010	2	1	0.091	0.005	
2344-2818	23:44:38	-28:18:29	-5	17.46	0	2	8360	66	2.104	0.024	0	0	0.000	0.000	1	3	-0.133	0.015	
2344-2828	23:44:38	-28:28:15	-2	16.65	0	1	8792	70	2.049	0.033	0	0	0.000	0.000	1	0	-0.002	0.015	
ESO 471G014	23:44:39	-28:14:06	-5	14.20	0	2	8427	67	2.345	0.018	0	1	0.292	0.008	2	2	0.362	0.005	
PGC 072403	23:44:40	-28:24:08	-5	16.35	2	2	8915	44	2.176	0.016	2	1	0.268	0.010	2	3	0.110	0.008	
2344-2820	23:44:44	-28:20:26	-2	17.23	0	1	8338	67	2.014	0.032	0	1	0.000	0.000	3	1	-0.226	0.014	
2344-2815	23:44:46	-28:15:12	-2	16.70	0	1	7454	60	2.152	0.027	0	0	0.000	0.000	2	1	0.008	0.005	
IC 5353	23:44:52	-28:23:13	-5	14.20	1	2	8220	24	2.445	0.015	1	1	0.327	0.011	2	2	0.438	0.007	
2344-2819	23:44:54	-28:19:16	-2	17.13	0	1	8237	65	2.031	0.033	0	1	0.000	0.000	1	1	-0.098	0.015	
2345-2826	23:45:09	-28:26:27	-5	17.21	0	2	9529	78	2.215	0.021	0	1	0.290	0.010	7	3	0.041	0.005	
2345-2823	23:45:09	-28:23:08	-2	18.20	0	1	8152	65	1.809	0.042	0	0	0.000	0.000	5	1	-0.195	0.011	
ESO-LV4710191	23:45:11	-28:24:46	-2	13.72	0	1	8161	69	2.190	0.033	0	2	0.000	0.000	4	1	-0.042	0.015	
2345-2821	23:45:13	-28:21:52	-5	17.39	0	2	9789	80	1.802	0.042	0	0	0.000	0.000	2	3	-0.139	0.030	
PGC 072466	23:45:44	-28:30:36	-5	15.05	1	2	8079	47	2.502	0.012	1	1	0.329	0.002	3	3	0.360	0.005	
PGC 072469	23:45:45	-28:23:38	-2	15.46	0	1	8923	72	2.098	0.031	0	1	0.000	0.000	0	1	-0.047	0.011	
PGC 072476	23:45:50	-28:33:24	-2	15.85	1	1	8243	63	2.224	0.020	1	0	0.297	0.010	3	0	0.164	0.005	
IC 5362	23:49:01	-28:38:34	-2	13.75	0	1	8137	67	2.355	0.021	0	1	0.313	0.010	1	1	0.400	0.011	

Table 8. The cluster sample: Galaxies with peculiarities/problematical measurements

Name	α	δ	T	m_B	N_s^o	N_s^l	cz_{hel}	$\epsilon_{cz_{hel}}$	$\log \sigma$	$\epsilon_{\log \sigma}$	N_M^o	N_M^l	Mg2	ϵ_{Mg2}	N_d^o	N_d^l	$\log d_n$	$\epsilon_{\log d_n}$	Notes
(1)	(2)	(3)	(4)	(5)	(6)	(7)	(8)	(9)	(10)	(11)	(12)	(13)	(14)	(15)	(16)	(17)	(18)	(19)	(20)
Pisces																			
[SLH97] Z01047	01:04:12	+32:02:30	-5	15.55	0	1	5493	56	2.110	0.030	0	1	0.288	0.009	0	1	0.213	0.025	1
NGC 0380	01:04:32	+32:13:01	-2	14.05	0	1	4414	27	2.466	0.014	0	1	0.341	0.010	1	1	0.589	0.009	4, 9, 16
NGC 0382	01:04:38	+32:08:12	-5	14.20	0	1	5228	41	2.256	0.021	0	1	0.275	0.001	0	1	0.408	0.011	1
HMS0122+33																			
NGC 0508	01:20:52	+33:01:13	-5	14.54	0	1	5517	57	2.343	0.024	0	1	0.312	0.009	0	1	0.446	0.025	1
A262																			
NGC 0704	01:49:41	+35:52:50	-2	14.87	0	1	4724	46	2.194	0.024	0	1	0.288	0.007	0	1	0.377	0.025	1
A347																			
CGCG 538-064	02:21:35	+42:23:51	-5	14.31	0	1	5917	60	2.550	0.030	0	1	0.354	0.009	0	1	0.543	0.025	9
Perseus																			
NGC 1250	03:12:00	+41:10:00	-2	14.20	2	0	6163	12	2.355	0.018	2	0	0.293	0.004	1	0	0.610	0.009	4
NGC 1260	03:14:09	+41:13:20	-2	14.20	3	1	5753	14	2.301	0.011	1	1	0.247	0.011	1	1	0.547	0.005	9, 4
NGC 1270	03:15:42	+41:17:00	-5	14.40	2	1	5002	52	2.605	0.008	1	1	0.367	0.006	1	1	0.659	0.011	4, 9, 16
IC 1907	03:16:20	+41:24:02	-5	15.42	0	1	4453	34	2.395	0.027	0	0	0.000	0.000	0	1	0.470	0.011	9, 4, 16
A539																			
MCG +01-14-013	05:13:52	+06:26:59	-2	17.15	0	1	8672	70	2.166	0.033	0	1	0.230	0.011	2	1	0.077	0.005	1
CGCG 421-018 NED01	05:13:56	+06:23:54	-5	17.20	0	1	8675	70	2.352	0.023	0	1	0.293	0.012	2	1	0.263	0.005	1
CGCG 421-018 NED03	05:13:56	+06:22:59	-5	16.72	0	1	7741	62	2.263	0.019	0	1	0.296	0.010	2	1	0.081	0.005	1
0514+0626	05:14:26	+06:26:27	-2	16.83	0	1	10012	43	2.247	0.033	0	1	0.301	0.011	2	1	0.093	0.005	12, 10, 9
CGCG 421-021	05:14:37	+06:05:02	-2	16.58	0	1	9695	42	2.327	0.024	0	1	0.289	0.008	1	1	0.397	0.005	12, 9, 2, 16
A1367																			
NGC 3837	11:41:20	+20:10:21	-5	14.20	1	2	6323	35	2.398	0.013	1	1	0.317	0.010	0	1	0.360	0.011	9, 4
IC 2955	11:42:31	+19:53:00	-5	14.93	0	1	6345	52	2.290	0.024	0	1	0.287	0.008	1	1	0.247	0.023	1
Virgo																			
IC 0719	11:37:42	+09:17:00	-2	13.60	2	0	1841	33	2.064	0.024	2	0	0.187	0.002	1	0	0.510	0.008	4, 7, 16
NGC 4078	12:02:12	+10:52:00	-2	13.90	1	0	2559	34	2.315	0.021	1	0	0.273	0.008	1	0	0.540	0.005	4, 16
NGC 4124	12:05:36	+10:40:00	-2	12.68	1	0	1645	28	1.943	0.039	1	0	0.118	0.011	1	0	0.610	0.008	6, 7, 11, 9
NGC 4191	12:11:18	+07:28:00	-2	13.90	1	0	2653	32	2.132	0.067	1	0	0.276	0.011	1	0	0.530	0.011	9, 4, 16
NGC 4215	12:13:24	+06:41:00	-2	13.04	1	0	2032	35	2.122	0.054	1	0	0.241	0.009	2	0	0.710	0.006	4
NGC 4233	12:14:36	+07:54:00	-2	13.41	1	0	2331	36	2.329	0.023	1	0	0.310	0.009	1	0	0.730	0.007	4, 6, 2, 16
NGC 4259	12:16:48	+05:39:00	-2	14.50	0	1	2492	29	2.193	0.029	0	1	0.000	0.000	1	0	0.410	0.006	4, 16
NGC 4261	12:16:48	+06:06:00	-5	11.84	0	3	2200	27	2.500	0.013	0	1	0.000	0.000	0	1	0.980	0.011	9, 16
NGC 4281	12:17:48	+05:40:00	-2	12.41	0	1	2732	26	2.462	0.018	0	1	0.000	0.000	1	0	0.870	0.014	4, 16
NGC 4292	12:18:42	+04:52:00	-2	14.10	0	1	2258	27	1.740	0.039	0	1	0.000	0.000	1	0	0.440	0.006	4, 5, 14, 16
NGC 4309	12:19:42	+07:25:00	-2	14.30	1	0	1028	33	2.101	0.031	1	0	0.178	0.009	1	0	0.230	0.008	9, 15
NGC 4324	12:20:36	+05:32:00	-2	12.60	2	1	1650	32	1.979	0.020	2	0	0.239	0.008	1	0	0.820	0.007	6, 4
NGC 4342	12:21:06	+07:19:51	-3	13.91	0	1	714	34	2.387	0.026	0	1	0.304	0.009	0	1	0.730	0.011	9, 7, 4
NGC 4340	12:21:04	+17:00:00	-2	12.25	0	3	932	28	2.057	0.018	0	0	0.000	0.000	1	0	0.770	0.007	5
NGC 4352	12:21:30	+11:30:00	-2	14.00	1	0	2099	22	1.930	0.040	1	0	0.185	0.011	1	0	0.500	0.005	4, 1
NGC 4371	12:22:24	+11:59:00	-2	12.25	0	2	941	28	2.119	0.029	0	0	0.000	0.000	2	0	0.940	0.007	5, 4, 8
NGC 4425	12:24:42	+13:00:42	-2	13.21	1	0	1898	22	1.790	0.038	1	0	0.237	0.011	1	0	0.660	0.008	6, 4, 5
NGC 4429	12:24:54	+11:23:00	-2	11.43	0	2	1131	26	2.306	0.023	0	0	0.000	0.000	1	0	1.060	0.009	4, 6
NGC 4435	12:25:07	+13:21:24	-2	12.03	0	1	773	27	2.241	0.040	0	0	0.000	0.000	1	0	1.000	0.011	5, 7
NGC 4459	12:26:30	+14:15:00	-2	11.95	0	2	1215	29	2.231	0.037	0	0	0.000	0.000	1	0	1.050	0.009	11, 2
NGC 4467	12:26:58	+08:16:10	-5	15.07	1	2	1423	30	1.846	0.039	1	1	0.262	0.008	1	1	0.250	0.010	1, 14, 9
NGC 4476	12:27:28	+12:37:30	-3	13.51	0	1	1955	27	1.629	0.048	0	0	0.000	0.000	0	1	0.660	0.011	13, 11, 14
NGC 4482	12:27:41	+11:03:12	-5	14.20	2	0	1856	30	1.341	0.036	2	0	0.074	0.011	1	0	0.110	0.006	15, 14, 9, 5
NGC 4486B	12:28:00	+12:46:00	-7	14.50	0	1	1586	47	2.221	0.027	0	0	0.000	0.000	1	1	0.560	0.010	13, 16

Table 8—Continued

Name	α	δ	T	m_B	N_s^o	N_s^l	cz_{hel}	$\epsilon_{cz_{hel}}$	$\log \sigma$	$\epsilon_{\log \sigma}$	N_M^o	N_M^l	Mg2	ϵ_{Mg2}	N_d^o	N_d^l	$\log d_n$	$\epsilon_{\log d_n}$	Notes
(1)	(2)	(3)	(4)	(5)	(6)	(7)	(8)	(9)	(10)	(11)	(12)	(13)	(14)	(15)	(16)	(17)	(18)	(19)	(20)
NGC 4486	12:28:17	+12:40:06	-3	10.30	1	2	1307	43	2.557	0.013	1	1	0.297	0.004	1	1	1.327	0.013	12, 6
NGC 4486A	12:28:24	+12:33:00	-5	11.20	1	0	150	45	1.614	0.043	1	0	0.036	0.011	3	0	0.713	0.005	15, 14
NGC 4526	12:31:30	+07:58:00	-2	10.97	0	1	602	27	2.508	0.018	0	0	0.000	0.000	2	0	1.180	0.006	4, 7
NGC 4552	12:33:06	+12:50:00	-5	11.30	0	1	322	28	2.410	0.031	0	1	0.325	0.010	0	1	1.150	0.011	12
NGC 4581	12:35:32	+01:45:00	-5	13.40	0	1	1818	29	2.165	0.028	0	0	0.000	0.000	0	1	0.600	0.011	16
NGC 4587	12:36:00	+02:56:00	-2	14.40	1	0	913	30	1.756	0.044	1	0	0.126	0.011	1	0	0.340	0.010	15, 14, 4
NGC 4596	12:37:24	+10:27:00	-2	11.88	0	2	1870	27	2.158	0.017	0	0	0.000	0.000	1	0	0.970	0.005	5
NGC 4598	12:37:42	+08:39:00	-2	14.10	0	1	1961	26	1.978	0.037	0	0	0.000	0.000	2	0	0.193	0.006	9, 5, 13
NGC 4608	12:38:42	+10:26:00	-2	12.48	0	1	1864	25	2.212	0.069	0	0	0.000	0.000	1	0	0.860	0.008	5
NGC 4612	12:39:00	+07:35:00	-2	12.59	1	0	1781	40	1.784	0.039	1	0	0.214	0.011	1	0	0.800	0.013	9, 14
IC 3773	12:44:44	+10:28:36	-5	14.30	1	0	1124	37	1.900	0.039	1	0	0.142	0.011	1	0	0.210	0.006	4, 14, 8
NGC 4694	12:45:42	+11:15:00	-2	12.64	1	0	1189	19	1.784	0.046	1	0	0.117	0.011	1	0	0.690	0.008	9, 8, 15
NGC 4710	12:47:06	+15:26:00	-2	12.28	1	0	1120	33	2.138	0.032	3	0	0.192	0.007	1	0	0.870	0.011	6, 7, 4
NGC 4866	12:57:00	+14:27:00	-2	12.36	1	0	1959	32	2.271	0.031	1	0	0.304	0.009	0	2	0.060	0.007	7, 4, 12
Coma																			
NGC 4789	12:51:53	+27:20:19	-5	13.42	0	2	8367	68	2.435	0.018	0	1	0.295	0.009	0	2	0.553	0.034	2
NGC 4841	12:55:06	+28:45:00	-2	14.00	0	1	6784	34	2.378	0.038	0	1	0.000	0.000	1	0	0.520	0.011	1, 9
NGC 4841B	12:55:09	+28:45:06	-5	13.77	0	1	6793	44	2.375	0.028	0	1	0.305	0.009	0	2	0.431	0.030	1, 9
NGC 4864	12:56:48	+28:14:54	-5	14.80	0	2	6760	54	2.301	0.020	0	2	0.287	0.001	0	3	0.346	0.011	1
NGC 4867	12:56:50	+28:14:24	-5	15.50	0	1	4818	52	2.364	0.030	0	0	0.000	0.000	0	2	0.282	0.005	1
IC 3976	12:57:04	+28:07:10	-2	16.53	1	0	6764	30	2.412	0.018	1	0	0.325	0.011	3	0	0.233	0.005	10, 4
NGC 4871	12:57:05	+28:13:31	-2	15.10	0	1	6837	54	2.249	0.032	0	1	0.282	0.010	0	3	0.232	0.011	1, 4
1257+2803	12:57:06	+28:03:45	-5	16.84	0	1	7833	44	1.916	0.036	0	1	0.240	0.011	0	1	-0.070	0.011	10, 14
NGC 4872	12:57:10	+28:13:09	-5	14.65	0	2	7145	25	2.334	0.018	0	2	0.300	0.002	1	3	0.280	0.006	1
PGC 044644	12:57:15	+28:13:32	-2	16.40	0	2	8001	62	2.029	0.022	0	2	0.247	0.005	0	4	-0.027	0.015	1
PGC 044652	12:57:19	+28:13:39	-2	17.32	1	0	7099	50	2.141	0.030	1	0	0.163	0.009	1	2	-0.119	0.021	10, 15
PGC 044675	12:57:31	+28:11:57	-2	17.33	1	0	7812	23	2.003	0.056	1	0	0.260	0.008	2	0	-0.190	0.015	4
NGC 4886	12:57:40	+28:15:32	-5	15.05	0	2	6218	49	2.206	0.014	0	1	0.254	0.002	0	4	0.247	0.005	4
NGC 4898 NED01	12:57:53	+28:13:35	-5	14.60	0	1	6848	56	2.318	0.021	0	1	0.270	0.010	0	1	0.500	0.011	1
NGC 4895	12:57:53	+28:28:27	-2	15.32	0	2	8446	68	2.335	0.018	0	2	0.288	0.004	0	2	0.469	0.011	4
NGC 4898 NED02	12:57:54	+28:13:41	-5	15.92	0	1	6349	52	2.162	0.031	0	1	0.258	0.010	0	1	0.110	0.011	1
IC 4042	12:58:18	+28:14:25	-2	16.99	0	2	6255	51	2.121	0.025	0	2	0.244	0.005	0	2	0.074	0.011	1, 4
HG50																			
NGC 5846A	15:03:56	+01:47:12	-5	14.10	0	1	2240	44	2.375	0.016	0	0	0.000	0.000	1	0	1.040	0.008	1
A2199																			
CGCG 224-034 NED01	16:26:14	+39:21:46	-2	15.70	0	1	8964	84	2.337	0.021	0	1	0.324	0.006	0	1	0.175	0.025	1
NGC 6661A NED01	16:26:48	+39:37:48	-2	16.14	0	2	10177	82	2.441	0.017	0	1	0.325	0.008	0	2	0.263	0.011	1
MCG +07-34-054	16:26:51	+39:39:29	-5	16.89	0	3	9824	43	2.109	0.018	0	2	0.269	0.004	0	3	-0.061	0.011	1
PGC 058257	16:26:53	+39:39:45	-5	17.56	0	2	8987	43	2.225	0.017	0	1	0.302	0.009	0	2	-0.193	0.027	1
NGC 6166	16:26:55	+39:39:37	-5	13.01	0	1	9284	44	2.496	0.012	0	1	0.328	0.007	0	2	0.418	0.005	1
CGCG 224-040 NED01	16:27:03	+39:34:19	-5	16.73	0	2	7872	63	2.161	0.022	0	1	0.274	0.012	0	2	0.039	0.011	1, 4
PGC 058309	16:27:17	+39:47:33	-5	16.33	0	2	8456	44	2.290	0.020	0	2	0.306	0.006	0	2	0.075	0.011	10, 9
Pegasus																			
NGC 7617	23:17:36	+07:53:00	-2	14.64	0	1	4072	34	2.162	0.027	0	1	0.227	0.009	0	1	0.240	0.011	1
A2634																			
NGC 7720 NED01	23:36:00	+26:45:14	-5	13.47	0	1	9141	65	2.509	0.015	0	1	0.331	0.011	1	1	0.518	0.012	1, 9
2336+2645	23:36:03	+26:45:29	-5	17.43	0	2	9828	79	2.249	0.020	0	1	0.297	0.009	0	2	0.040	0.011	1
A194																			
CGCG 385-098	01:21:08	-02:05:28	-2	15.94	0	1	5592	40	2.036	0.032	0	1	0.297	0.011	0	1	0.193	0.011	12

Table 8—Continued

Name	α	δ	T	m_B	N_s^o	N_s^l	cz_{hel}	$\epsilon_{cz_{hel}}$	$\log \sigma$	$\epsilon_{\log \sigma}$	N_M^o	N_M^l	Mg2	ϵ_{Mg2}	N_d^o	N_d^l	$\log d_n$	$\epsilon_{\log d_n}$	Notes
(1)	(2)	(3)	(4)	(5)	(6)	(7)	(8)	(9)	(10)	(11)	(12)	(13)	(14)	(15)	(16)	(17)	(18)	(19)	(20)
0122-0131	01:22:21	-01:31:03	-2	17.52	0	1	5072	25	1.954	0.032	0	1	0.000	0.000	3	0	-0.200	0.015	10, 4
CGCG 385-127	01:23:14	-01:36:14	-2	15.82	0	3	5535	42	2.109	0.018	0	1	0.244	0.009	6	3	0.235	0.005	9, 4
NGC 0545	01:23:24	-01:36:00	-3	13.70	2	7	5408	63	2.404	0.008	2	2	0.324	0.006	3	3	0.610	0.005	1
NGC 0547	01:23:30	-01:36:00	-5	13.40	1	6	5521	18	2.401	0.009	1	2	0.328	0.005	2	3	0.596	0.005	1
IC 0120	01:25:40	-02:10:40	-2	15.36	0	1	4806	39	2.058	0.031	0	1	0.247	0.010	0	1	0.223	0.011	6, 4
Fornax																			
MCG -06-08-019	03:25:20	-34:42:00	-5	14.30	2	0	1253	31	1.664	0.032	2	0	0.152	0.011	2	1	0.182	0.030	2, 13, 14, 11
NGC 1341	03:26:04	-37:19:24	-3	13.21	1	0	1857	33	1.905	0.032	1	0	0.119	0.011	1	0	0.460	0.006	4
MCG -06-08-27	03:32:34	-35:42:45	-5	14.81	1	0	1294	31	2.162	0.018	1	0	0.149	0.008	2	0	-0.765	0.020	11
ESO 358G029	03:34:36	-35:27:37	-2	12.60	1	1	1725	26	2.182	0.025	1	0	0.257	0.009	2	0	0.840	0.006	4
MCG -06-09-08	03:34:59	-35:32:19	-2	14.77	1	0	1710	30	1.779	0.045	1	0	0.187	0.011	3	0	0.133	0.006	13, 14
NGC 1396	03:36:12	-35:36:09	-3	14.82	1	0	836	34	1.812	0.043	1	0	0.122	0.011	2	0	-0.270	0.030	11, 1
IC 2006	03:52:36	-36:06:48	-3	12.53	1	3	1355	33	2.093	0.017	1	2	0.278	0.008	0	2	0.787	0.005	12
Eridanus																			
ESO 548G033	03:30:13	-19:06:54	-2	14.10	1	0	1652	32	1.858	0.042	1	0	0.164	0.011	1	0	0.280	0.005	4, 2
ESO 548G048	03:33:01	-20:32:18	-2	13.70	2	0	1035	32	1.840	0.040	2	0	0.093	0.011	3	0	0.427	0.008	9, 1, 12
ESO 548G051	03:34:26	-21:03:54	-2	13.70	1	0	1760	36	1.916	0.036	1	0	0.091	0.011	2	2	0.586	0.030	11, 13, 7
ESO 548G053	03:35:23	-18:30:06	-2	14.00	1	0	1939	34	2.237	0.035	1	0	0.226	0.010	1	0	0.640	0.008	4
ESO 548G058	03:36:23	-18:35:24	-2	13.80	1	0	2127	29	2.049	0.034	1	0	0.209	0.009	1	0	0.620	0.011	4
ESO 548G066	03:37:52	-18:36:18	-2	14.10	1	0	1813	31	1.911	0.036	1	0	0.164	0.011	3	0	0.270	0.006	4
ESO 482G034	03:38:52	-22:52:42	-2	14.26	1	0	2137	35	2.243	0.023	1	0	0.172	0.009	0	1	0.620	0.011	13, 2
ESO 482G029	03:38:23	-27:01:18	-2	13.90	1	0	1770	20	1.886	0.037	1	0	0.226	0.011	2	0	0.605	0.005	4
ESO 549G007	03:41:57	-19:28:36	-2	14.40	1	0	1527	33	1.713	0.044	0	1	0.000	0.000	3	0	-0.730	0.028	4, 14
NGC 1461	03:46:12	-16:32:00	-2	13.50	1	1	1460	31	2.312	0.021	1	0	0.262	0.009	1	0	0.800	0.005	7, 15, 4
Doradus																			
ESO 249G011	03:37:04	-44:15:42	-2	11.96	0	1	998	22	2.095	0.040	0	1	0.213	0.011	0	1	0.883	0.011	12, 2
ESO 250G005	04:03:02	-46:10:42	-2	14.00	3	0	1231	30	1.806	0.042	3	0	0.064	0.011	0	1	-0.297	0.011	12, 9, 4
ESO 157G003	04:08:46	-56:15:00	-2	12.14	0	1	823	26	2.259	0.022	0	1	0.282	0.011	0	1	0.903	0.011	4, 5, 12
ESO 118G010	04:11:44	-57:51:48	-2	11.83	0	1	1088	23	2.155	0.030	0	1	0.277	0.010	1	1	0.974	0.006	5, 4
ESO 157G017	04:15:05	-55:54:12	-2	10.73	0	1	1270	25	2.237	0.032	0	1	0.264	0.011	2	1	1.257	0.007	4, 12, 13
ESO 157G031	04:26:32	-55:08:12	-2	12.16	0	1	1533	27	2.222	0.035	0	1	0.271	0.011	0	1	0.913	0.011	4, 12
A3381																			
PGC 018509	06:07:44	-33:49:53	-2	16.24	1	1	11279	32	2.255	0.028	1	1	0.324	0.011	0	1	0.033	0.011	10, 13
PGC 018526	06:08:03	-33:40:44	-2	15.00	0	1	11154	53	1.979	0.059	0	1	0.210	0.011	0	1	-0.357	0.055	11
PGC 018529	06:08:08	-33:32:29	-5	17.07	0	1	11335	40	2.217	0.025	0	1	0.283	0.008	1	1	-0.086	0.030	1, 11
PGC 018531	06:08:10	-33:32:19	-2	16.00	0	1	11255	32	2.061	0.028	0	1	0.251	0.013	0	1	-0.062	0.033	1
0608-3326	06:08:28	-33:26:48	-2	15.00	0	1	11213	28	2.123	0.025	0	1	0.243	0.018	0	1	-0.002	0.030	10, 11
ESO 364IG042	06:09:17	-33:17:38	-2	15.44	0	1	11488	92	2.332	0.032	0	1	0.284	0.011	1	1	0.214	0.006	1
PGC 018592	06:09:50	-33:06:39	-3	15.12	0	1	11059	89	2.369	0.027	0	1	0.288	0.009	1	1	0.251	0.005	6
Hydra																			
ESO 436G030	10:28:43	-28:27:42	-5	13.94	1	0	3678	30	2.526	0.019	1	0	0.322	0.009	2	0	0.610	0.006	13
ESO 501G021	10:32:59	-27:06:10	-2	14.41	0	1	4592	37	2.174	0.035	0	1	0.000	0.000	1	1	0.410	0.010	4
ESO 501G027	10:33:37	-27:03:35	-5	15.25	1	2	3206	32	1.858	0.039	1	1	0.177	0.011	0	1	-0.107	0.011	9, 4, 15
ESO 501G028	10:33:41	-24:03:48	-3	13.65	1	0	3547	30	2.353	0.022	1	0	0.335	0.011	2	0	0.545	0.005	13, 16
D154	10:34:14	-27:12:37	-5	15.91	0	2	3193	41	2.097	0.020	0	0	0.000	0.000	1	2	-0.007	0.030	11, 10
ESO 501G038	10:34:22	-27:16:06	-2	12.19	1	5	3833	33	2.269	0.011	1	2	0.314	0.010	2	4	0.558	0.011	6, 9, 1
ESO 437G015	10:34:37	-27:55:06	-2	13.81	1	0	2765	12	2.226	0.024	1	0	0.180	0.012	1	0	0.650	0.006	4
PGC 031515	10:34:43	-27:08:24	-2	14.60	0	2	2710	22	2.083	0.025	0	0	0.000	0.000	0	2	0.226	0.008	2
ESO 501G054	10:35:16	-27:20:03	-2	13.92	2	3	3941	15	2.275	0.013	2	1	0.285	0.005	3	2	0.519	0.008	5

Table 8—Continued

Name	α	δ	T	m_B	N_s^o	N_s^l	cz_{hel}	$\epsilon_{cz_{hel}}$	$\log \sigma$	$\epsilon_{\log \sigma}$	N_M^o	N_M^l	Mg2	ϵ_{Mg2}	N_d^o	N_d^l	$\log d_n$	$\epsilon_{\log d_n}$	Notes
(1)	(2)	(3)	(4)	(5)	(6)	(7)	(8)	(9)	(10)	(11)	(12)	(13)	(14)	(15)	(16)	(17)	(18)	(19)	(20)
[RMH82] 50	10:35:20	-26:47:02	-2	17.48	0	1	3075	24	1.966	0.042	0	1	0.244	0.011	1	1	0.044	0.005	13
ESO 437G027	10:36:21	-28:30:36	-2	15.42	2	0	3684	33	1.648	0.051	2	0	0.168	0.011	1	0	-0.120	0.015	4, 7, 13, 14
AS639																			
ESO 264G024	10:37:02	-45:52:48	-3	14.12	0	1	6099	40	2.373	0.022	0	1	0.273	0.011	1	1	0.654	0.005	4, 7, 3
1037-4605	10:37:54	-46:05:24	-5	—	0	1	5852	44	2.092	0.032	0	1	0.253	0.020	0	1	0.138	0.009	1, 3
ESO 264IG030 NED03	10:38:06	-46:03:59	-2	14.57	0	2	5358	43	2.269	0.016	0	1	0.280	0.010	1	1	0.378	0.005	1
ESO 264IG030 NED02	10:38:09	-46:03:49	-2	16.35	0	1	6482	43	2.280	0.023	0	1	0.262	0.009	0	1	0.348	0.007	1
Cen45																			
MCG -07-26-057	12:47:21	-41:07:31	-5	14.40	0	2	4957	41	2.029	0.022	0	1	0.265	0.012	0	2	0.391	0.008	1, 16
ESO 323G024	12:49:44	-38:52:30	-5	13.12	0	1	4277	21	2.403	0.028	0	1	0.297	0.009	0	1	0.810	0.011	4, 7
Cen30																			
ESO 322G006	12:22:39	-39:29:00	-2	11.85	0	1	3415	22	2.385	0.017	0	1	0.000	0.000	0	2	0.973	0.005	16, 9, 1
ESO 322G030	12:33:26	-39:09:48	-2	13.57	1	0	3102	30	2.191	0.026	1	0	0.308	0.009	1	0	0.680	0.006	4, 7
ESO 322G049	12:38:00	-40:29:18	-2	14.42	2	0	3134	21	1.960	0.019	2	0	0.256	0.009	1	0	0.540	0.008	7, 4
ESO 322G059	12:40:21	-41:05:06	-2	13.71	1	1	3265	31	2.354	0.017	2	1	0.290	0.009	1	1	0.580	0.030	6, 4, 7
NGC 4677	12:44:12	-41:18:36	-2	13.77	1	0	3107	30	2.009	0.039	1	0	0.250	0.012	1	0	0.590	0.008	4, 7
ESO 322G083	12:44:57	-41:15:18	-2	14.28	1	0	3570	17	2.122	0.033	1	0	0.282	0.013	1	0	0.600	0.008	5, 4
ESO 322G088	12:45:36	-41:26:30	-2	14.28	0	1	2650	22	2.222	0.018	0	1	0.273	0.011	0	1	0.650	0.008	4, 9
ESO 322G102	12:46:52	-41:06:59	-2	14.58	1	2	3684	12	2.009	0.021	1	0	0.236	0.011	0	2	0.468	0.008	4
ESO 322G101	12:46:48	-40:47:00	-5	14.16	0	2	2040	43	2.218	0.021	0	1	0.310	0.010	0	2	0.492	0.013	16, 3
ESO 323G005	12:47:26	-41:14:36	-2	14.25	0	2	2384	22	2.314	0.019	0	2	0.000	0.000	0	2	0.648	0.008	4
PGC 043506	12:48:14	-41:27:06	-5	15.19	0	1	2459	44	2.222	0.031	0	1	0.216	0.010	0	1	0.261	0.011	16, 10, 3
ESO 323G019	12:49:17	-41:11:18	-3	14.36	0	1	3739	25	2.109	0.024	0	1	0.250	0.011	0	1	0.580	0.008	5, 3
ESO 381G029	12:53:43	-36:06:00	-5	13.89	2	0	2641	31	2.049	0.021	2	0	0.194	0.011	0	1	0.374	0.011	12, 2
ESO 323IG079	13:03:52	-38:00:30	-3	14.08	2	0	3381	30	2.104	0.014	2	0	0.256	0.011	1	0	0.510	0.006	9, 4
ESO 323G089	13:07:46	-39:20:24	-2	13.88	0	1	2937	21	2.375	0.014	0	1	0.000	0.000	0	1	0.650	0.008	4
AS714																			
ESO 507G024	12:48:46	-26:32:06	-2	13.96	2	0	3407	30	2.067	0.015	2	0	0.225	0.008	1	0	0.490	0.006	5
Klemola27																			
NGC 5291	13:44:33	-30:09:37	-2	13.30	12	0	4289	74	2.282	0.011	12	0	0.237	0.011	1	1	0.618	0.008	9, 1
MCG -05-33-011	13:45:23	-30:18:08	-2	14.37	2	0	4264	33	2.011	0.023	2	0	0.231	0.011	1	1	0.318	0.030	9, 4, 11
ESO 445G042	13:45:57	-30:54:26	-2	14.35	2	0	5144	14	2.087	0.014	2	0	0.228	0.009	1	0	0.400	0.005	7, 4
ESO 445G043	13:45:58	-30:15:46	-2	13.28	1	0	3572	30	2.351	0.027	1	0	0.287	0.009	3	0	0.627	0.006	4
[WFC91] 050	13:46:15	-30:34:16	-5	14.71	2	0	4866	30	1.768	0.036	2	0	0.169	0.011	0	1	0.283	0.011	4, 14
ESO 445G049	13:46:17	-30:55:00	-2	13.80	2	0	5002	29	2.289	0.019	2	0	0.256	0.003	1	0	0.480	0.010	6, 7, 4
ESO 445G052	13:47:10	-30:19:48	-2	13.85	2	2	3749	33	2.338	0.014	2	2	0.263	0.011	1	2	0.547	0.005	12, 9, 1
ESO 445G054	13:47:41	-29:48:03	-2	14.97	0	1	5275	31	1.957	0.038	0	1	0.170	0.011	0	1	0.313	0.011	12, 4, 5
AS753																			
ESO 384G021	13:55:02	-33:45:55	-2	14.40	1	0	4340	36	2.039	0.049	1	0	0.268	0.009	1	0	0.410	0.006	5, 2
ESO 384G023	13:55:34	-33:59:58	-2	14.48	1	1	3927	62	2.076	0.024	1	1	0.225	0.009	1	1	0.391	0.005	4
ESO 384G029	13:57:51	-33:59:00	-2	14.16	2	1	3446	32	2.172	0.017	2	1	0.221	0.011	1	1	0.471	0.005	4
ESO 384G031	13:58:14	-33:42:12	-2	12.75	1	2	4138	36	2.432	0.010	1	2	0.305	0.006	1	2	0.569	0.008	6, 9
ESO 384G033	13:58:33	-34:00:03	-2	14.75	1	0	3735	21	1.899	0.039	1	0	0.226	0.011	1	0	0.240	0.008	5
[WFC91] 050	14:00:11	-33:33:53	-2	15.66	1	0	3933	48	2.248	0.060	1	0	0.244	0.012	1	1	0.041	0.009	10, 3, 16
ESO 384G037	14:00:38	-33:50:02	-2	14.78	3	0	5723	37	1.970	0.022	3	0	0.205	0.011	0	1	0.233	0.011	9, 4, 5
[WFC91] 068	14:01:12	-33:40:24	-5	16.56	1	0	4261	33	2.135	0.026	1	0	0.227	0.010	1	0	0.010	0.008	10, 13
[WFC91] 082	14:03:07	-34:04:20	-2	14.76	1	0	4537	34	1.964	0.035	1	0	0.272	0.011	0	1	0.273	0.011	5, 8
PavoII																			
IC 4751	18:38:42	-62:09:42	-2	14.08	1	0	4526	38	2.099	0.036	1	0	0.193	0.009	1	0	0.530	0.008	4, 5

Table 8—Continued

Name	α	δ	T	m_B	N_s^o	N_s^l	cz_{hel}	$\epsilon_{cz_{hel}}$	$\log \sigma$	$\epsilon_{\log \sigma}$	N_M^o	N_M^l	Mg2	ϵ_{Mg2}	N_d^o	N_d^l	$\log d_n$	$\epsilon_{\log d_n}$	Notes
(1)	(1950) (2)	(1950) (3)	(4)	mag (5)	(6)	(7)	kms^{-1} (8)	kms^{-1} (9)	(10)	(11)	(12)	(13)	(14)	(15)	(16)	(17)	(18)	(19)	(20)
IC 4767	18:42:57	-63:27:37	-2	14.85	0	3	3495	40	2.165	0.014	0	1	0.244	0.013	0	3	0.309	0.006	4, 6
NGC 6706	18:52:09	-63:13:54	-3	13.88	1	0	3837	31	2.334	0.026	1	0	0.208	0.010	1	0	0.490	0.008	6, 4
IC 4798	18:53:44	-62:11:12	-2	13.18	1	0	4511	23	2.330	0.022	1	0	0.251	0.010	1	0	0.720	0.008	9
NGC 6734	19:02:19	-65:32:24	-3	13.75	2	0	4288	15	2.208	0.019	2	0	0.290	0.011	1	0	0.500	0.006	1, 9
Klemola44																			
IC 5349 NED02	23:43:47	-28:16:50	-5	15.03	1	1	8648	30	2.171	0.019	1	0	0.272	0.011	3	0	0.113	0.012	1
2344-2823	23:44:47	-28:23:49	-2	14.88	0	2	9647	58	2.238	0.017	1	0	0.338	0.009	2	1	0.067	0.005	13
IC 5354	23:44:52	-28:24:50	-5	14.76	1	2	8325	77	2.443	0.015	1	1	0.306	0.011	2	3	0.367	0.005	1
PGC 072423	23:44:55	-28:23:06	-5	15.64	1	2	8429	23	2.239	0.018	1	1	0.329	0.011	2	3	0.173	0.005	1
PGC 072429	23:44:59	-28:24:11	-5	16.47	0	2	9185	68	2.077	0.025	0	1	0.283	0.013	3	2	0.079	0.021	13, 11
IC 5349 NED01	23:45:03	-28:17:25	-2	17.25	1	1	7927	32	1.973	0.025	1	0	0.255	0.011	2	0	-0.020	0.017	9
PGC 072437	23:45:07	-28:25:18	-2	15.61	0	1	8554	59	2.281	0.031	0	2	0.000	0.000	5	1	0.205	0.023	1
PGC 072436	23:45:07	-28:27:01	-5	16.32	0	2	8271	27	2.121	0.025	0	0	0.000	0.000	6	3	0.060	0.008	1, 14
IC 5358	23:45:08	-28:25:01	-2	13.78	0	2	8726	70	2.345	0.018	0	1	0.361	0.008	5	3	0.334	0.005	1
2345-2825a	23:45:26	-28:26:28	-2	16.27	0	1	9596	60	2.164	0.037	0	1	0.000	0.000	3	0	0.093	0.005	1
2345-2827	23:45:29	-28:27:20	-2	17.38	0	1	8314	40	2.083	0.030	0	0	0.000	0.000	4	1	-0.316	0.022	10, 11
PGC 072473	23:45:50	-28:28:03	-2	16.26	0	2	8964	72	2.140	0.020	0	1	0.000	0.000	4	1	0.153	0.005	1
2345-2825b	23:45:51	-28:25:40	-2	16.81	1	1	9263	11	1.953	0.025	1	0	0.261	0.011	0	1	-0.147	0.011	6
ESO 471G027	23:49:15	-28:14:36	-2	14.50	1	0	8803	10	2.140	0.035	1	0	0.186	0.009	1	0	-0.160	0.015	4, 7

Note. — The number in column (20) flags the following causes for features observed in the image and/or spectrum of a galaxy: (1) strong contamination by other galaxies along the line of sight, or interacting galaxies; (2) strong contamination by bright stars along the line of sight; (3) crowded background; (4) presence of spiral arms or shells; (5) presence of a bar; (6) presence of dust lanes; (7) high D/B ratio, edge-on galaxy; (8) evidence of star formation; (9) peculiar shape, peculiar nucleus, presence of spikes; (10) faint galaxy; (11) d_n available in the literature but uncertain or image problems: large masked region, saturation, large galaxy compared to the field-of-view; (12) presence of emission lines; (13) velocity dispersion available in the literature but uncertain or low S/N spectrum; (14) low velocity dispersion on the limit of the resolution; (15) peculiar spectrum (eg. broad lines) absorption lines too weak or undetectable; (16) probably not a cluster member.